Mechanistic Insights on CO_2 Utilization using Sustainable Catalysis

Abdussalam K. Qaroush,[*a] Areej K. Hasan,[a] Suhad B. Hammad,[a] Feda'a M. Al-Qaisi,[b] Khaleel I. Assaf,[c] Fatima Alsoubani[b] and Ala'a F. Eftaiha[*b]

[a] Department of Chemistry, Faculty of Science, The University of Jordan, Amman 11942, Jordan.
[b] Department of Chemistry, Faculty of Science, The Hashemite University, P.O. Box 330127, Zarqa 13133, Jordan.
[c] Department of Chemistry, Faculty of Science, Al-Balqa Applied University, 19117 Al-Salt, Jordan.

Supporting Information

Table S1. Elemental analysis for each caffeinium adduct.

	CAFH•Br		**CAFH•I•**H_2O		**CAFH•Cl•**$2H_2O$	
	Expected%	Found%	Expected%	Found%	Expected%	Found%
C	34.93	34.82	28.25	28.44	36.03	36.02
H	4.03	3.92	3.85	4.10	5.67	4.63
N	20.37	20.21	16.47	16.48	21.01	20.85

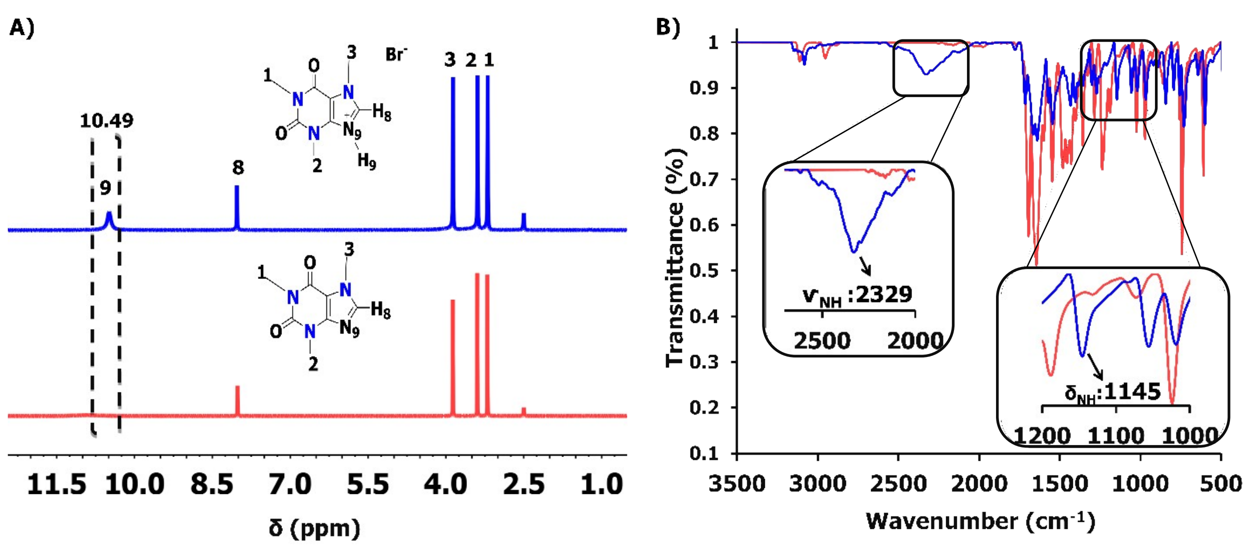

Figure S1. A. [1]H NMR spectra of the parent CAF molecule and its bromide adduct in DMSO-d_6, **B.** ATR-FTIR spectra of CAF (red trace) and **CAFH•Br** (blue trace).

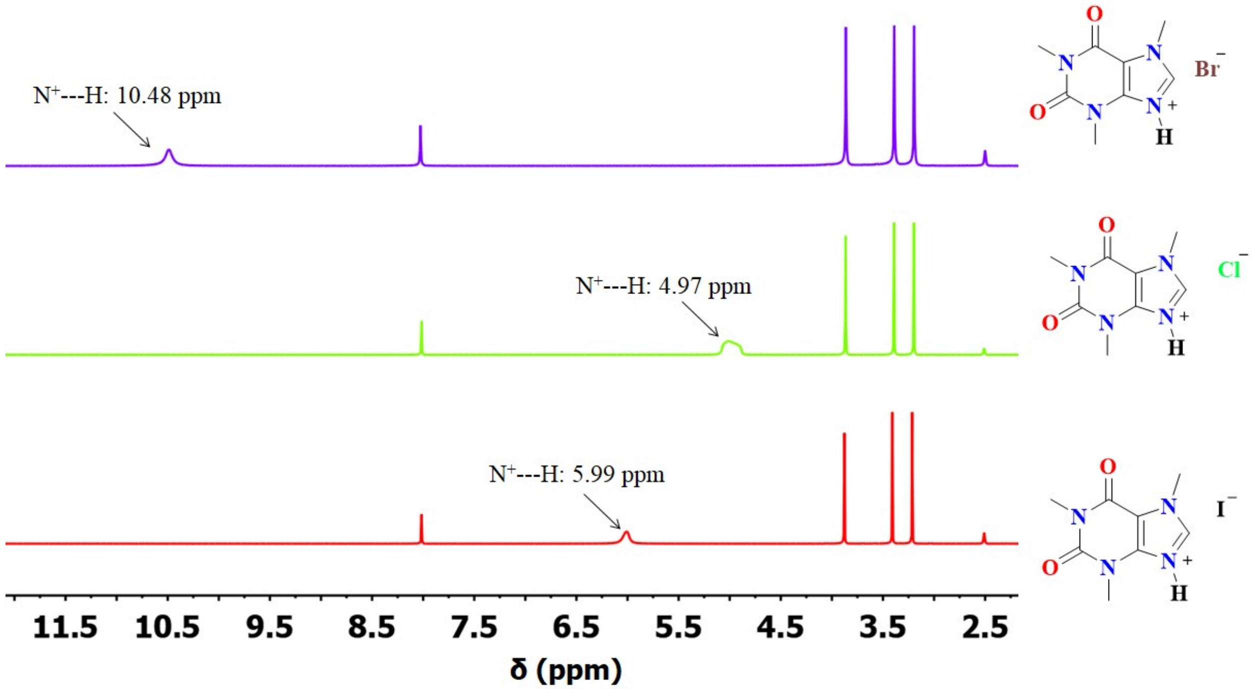

Figure S2. ^{1}H NMR spectra of caffeinium salts dissolved in DMSO-d_6.

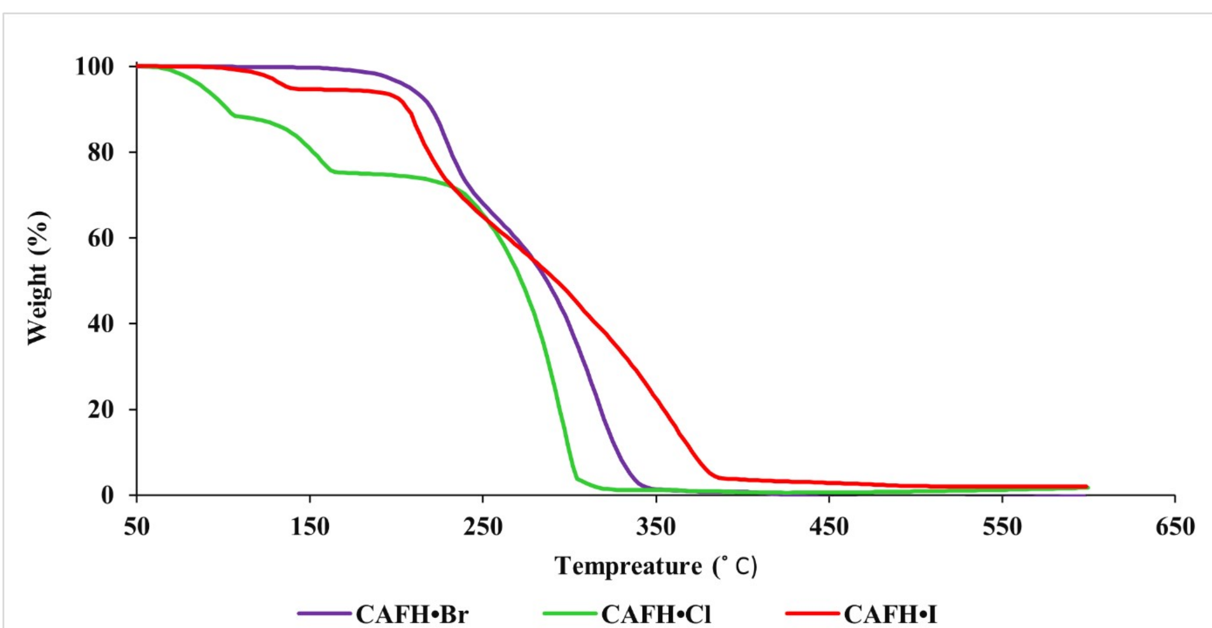

Figure S3. The TGA traces of the caffeinium adducts.

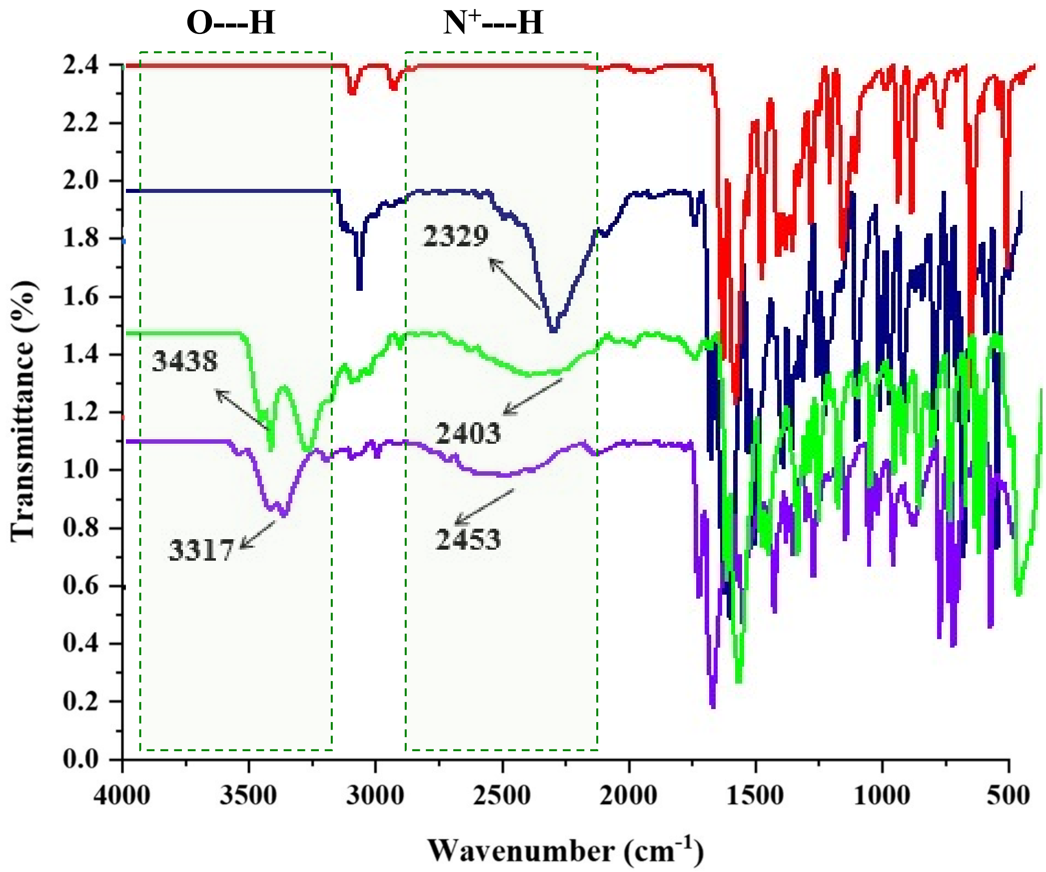

Figure S4. ATR-FTIR spectra of CAF (red trace), **CAFH•Br** (dark blue trace), **CAFH•Cl** (green trace), and **CAFH•I** (violet trace).

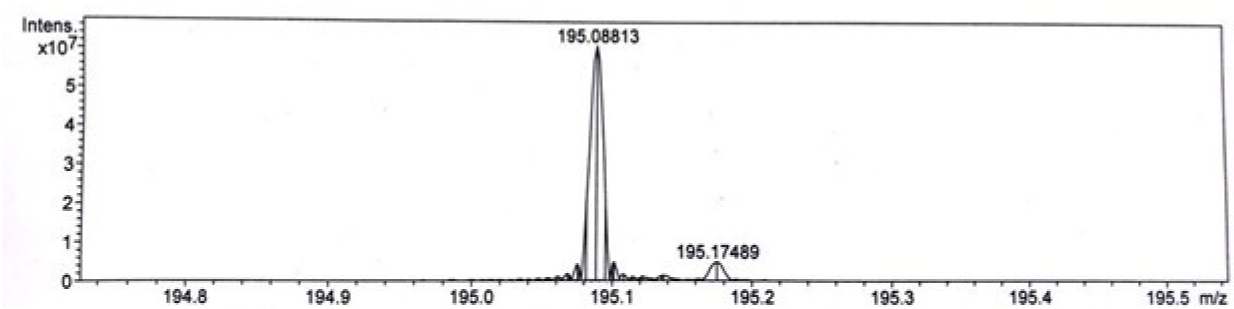

Figure S5. High-resolution mass spectrum of **CAFH•Br**, m/z of $[C_8H_{11}N_4O_2]^+$: 195.08813.

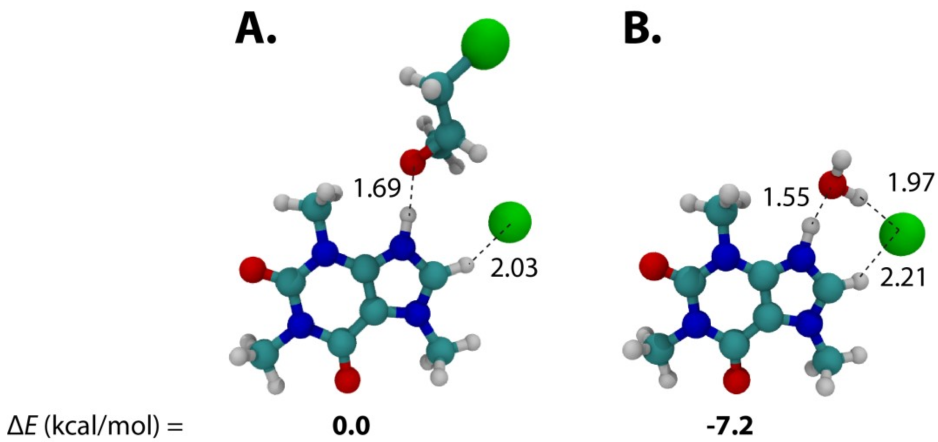

Figure S6. DFT-optimized molecular geometries of **A. CAFH•Cl**·ECH and **B. CAFH•Cl**·H_2O and their relative stabilization energy.

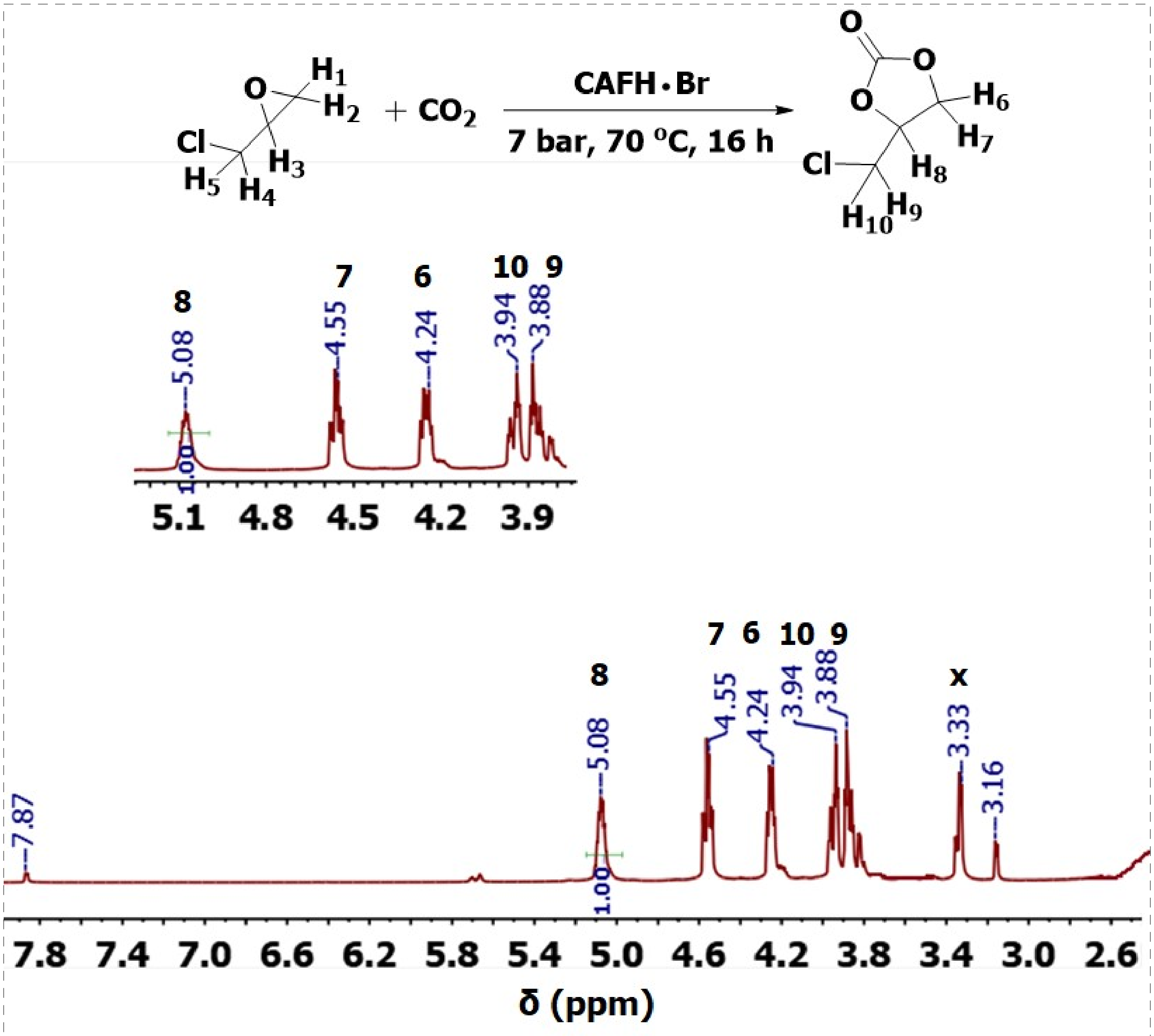

Figure S7. [1]H NMR spectrum of ECH conversion in DMSO-d_6, **x**: water, peaks at 3.17 and 7.87 ppm are corresponding to the catalyst (**Table 1**, Entry 1).

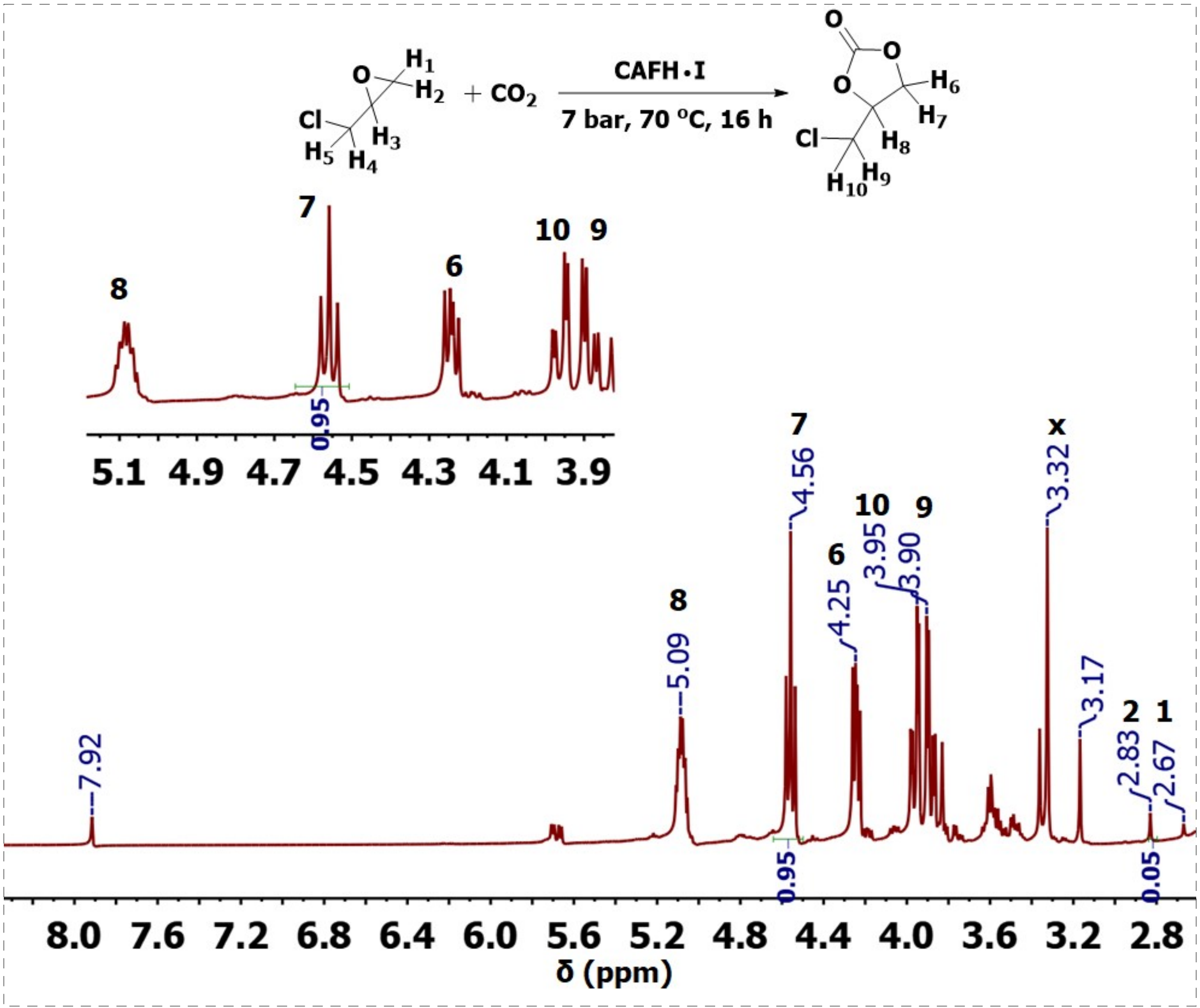

Figure S8. ^{1}H NMR spectrum of ECH conversion in DMSO-d_6, **x**: water, peaks at 3.17 and 7.92 ppm are corresponding to the catalyst (**Table 1**, Entry 2).

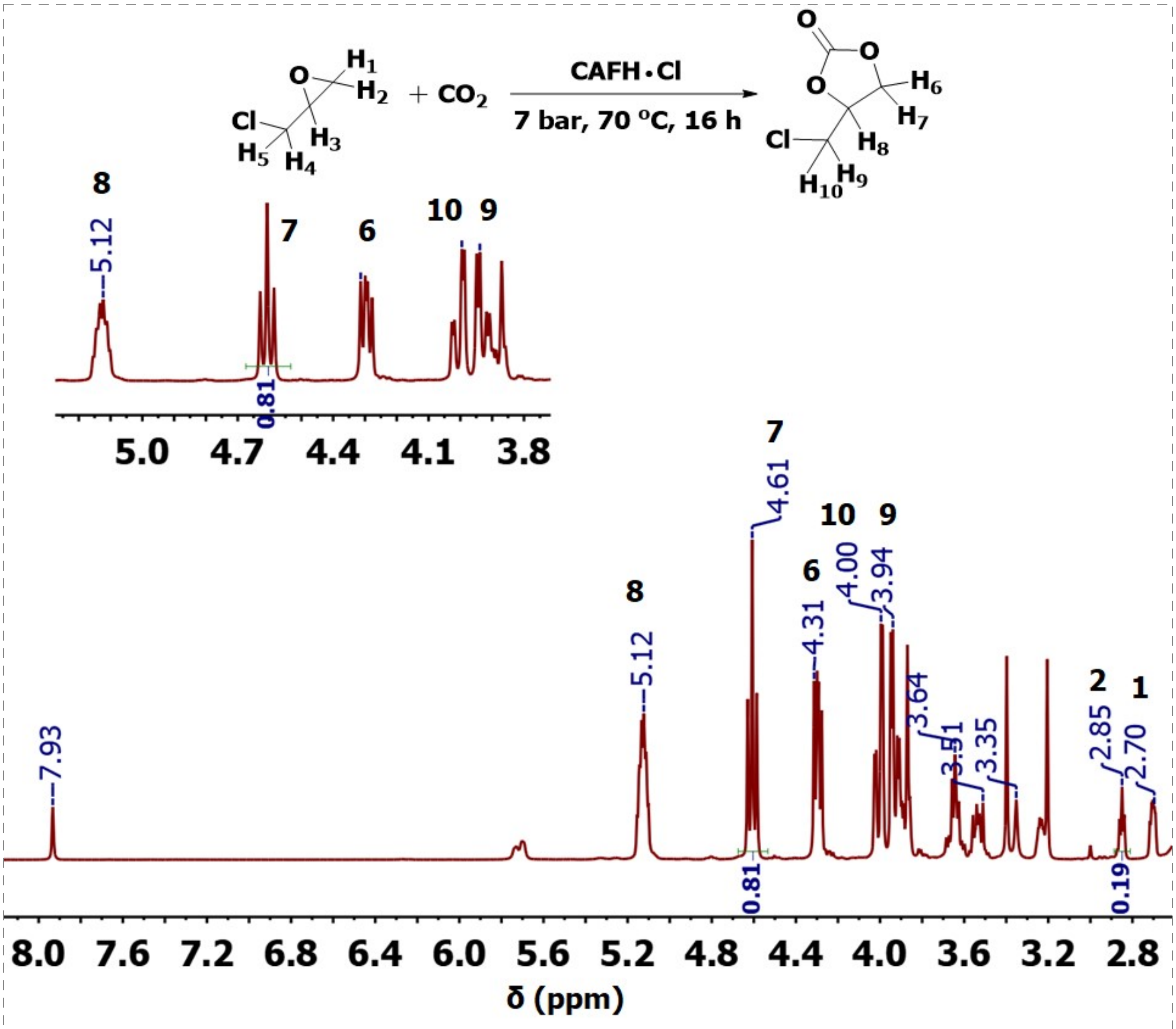

Figure S9. ^{1}H NMR spectrum of ECH conversion in DMSO-d_6, **x**: water, peak at 7.93 ppm is corresponding to the catalyst (**Table 1**, Entry 3).

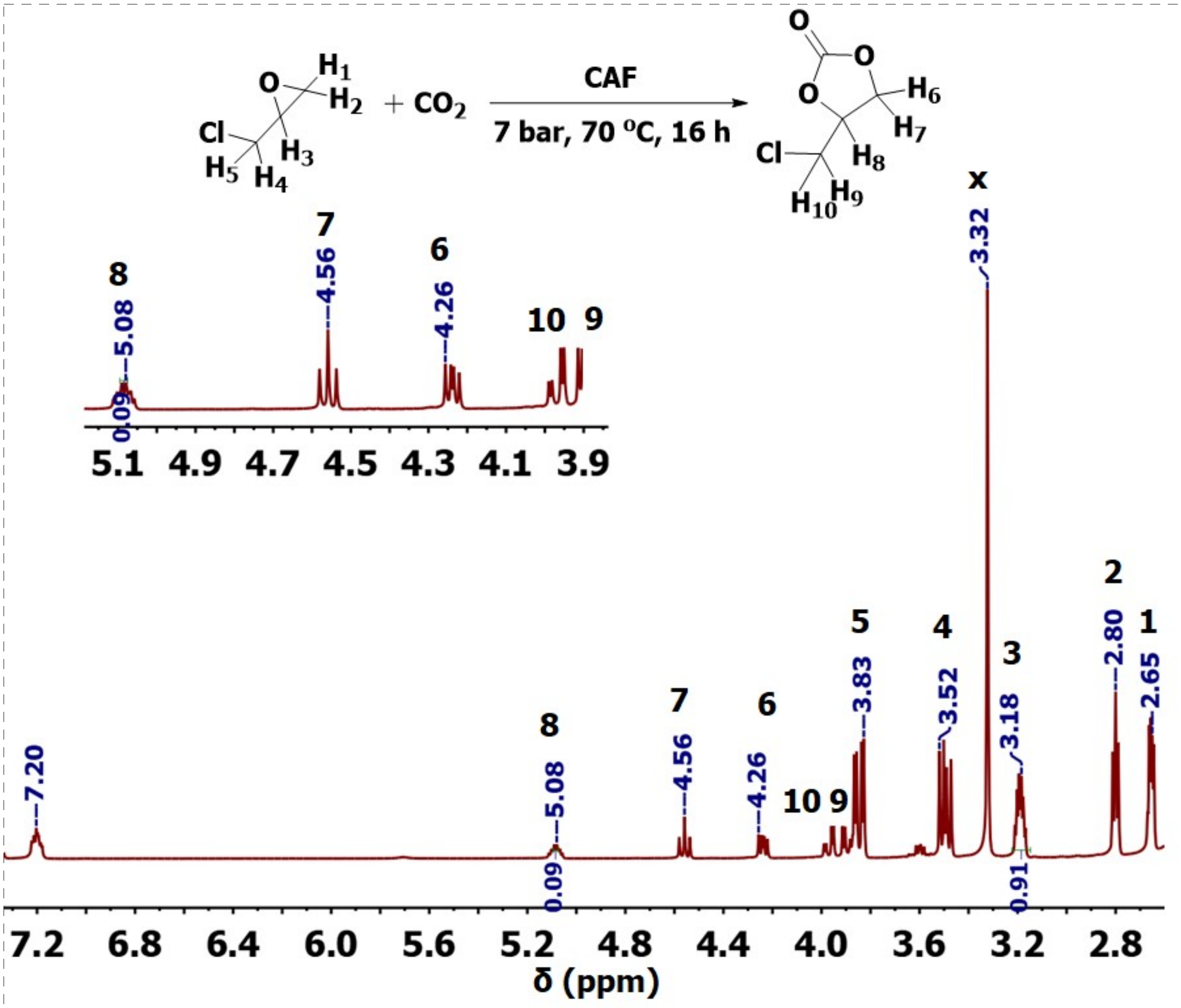

Figure S10. [1]H NMR spectrum of ECH conversion in DMSO-d_6, **x**: water, peak at 7.20 is corresponding to CAF (**Table 1**, Entry 4).

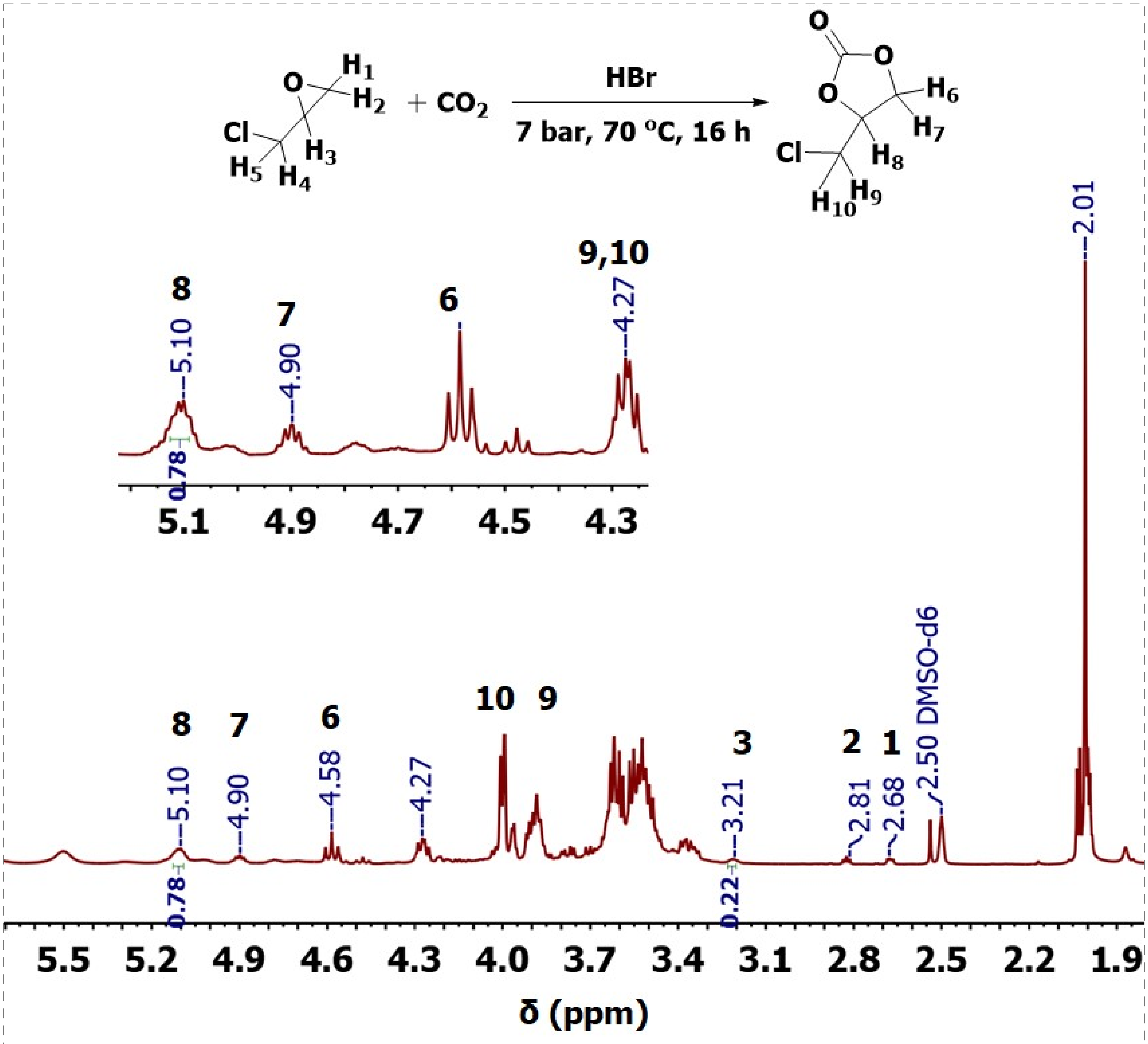

Figure S11. ^{1}H NMR spectrum of ECH conversion in DMSO-d_6, the peak at 2.01 ppm ascribed to the methyl group in acetic acid. HBr acid promoted the ring opening step upon the formation of halo-alcoholic compounds.[1,2] (**Table 1**, Entry 5).

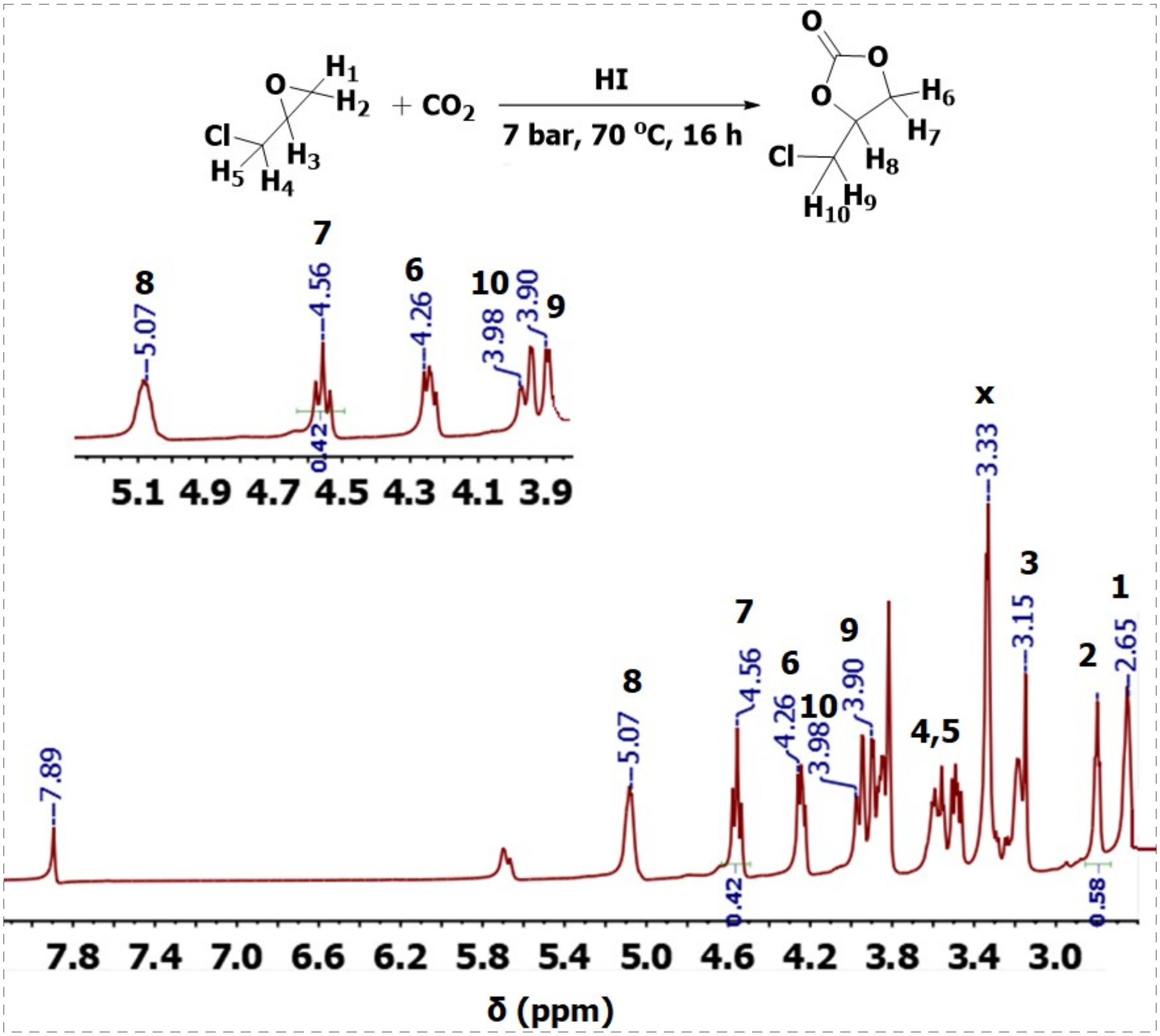

Figure S12. ^{1}H NMR spectrum of ECH conversion in DMSO-d_6, **x**: water. HI acid promoted the ring opening step upon the formation of halo-alcoholic compounds.[1,2] (**Table 1**, Entry 6).

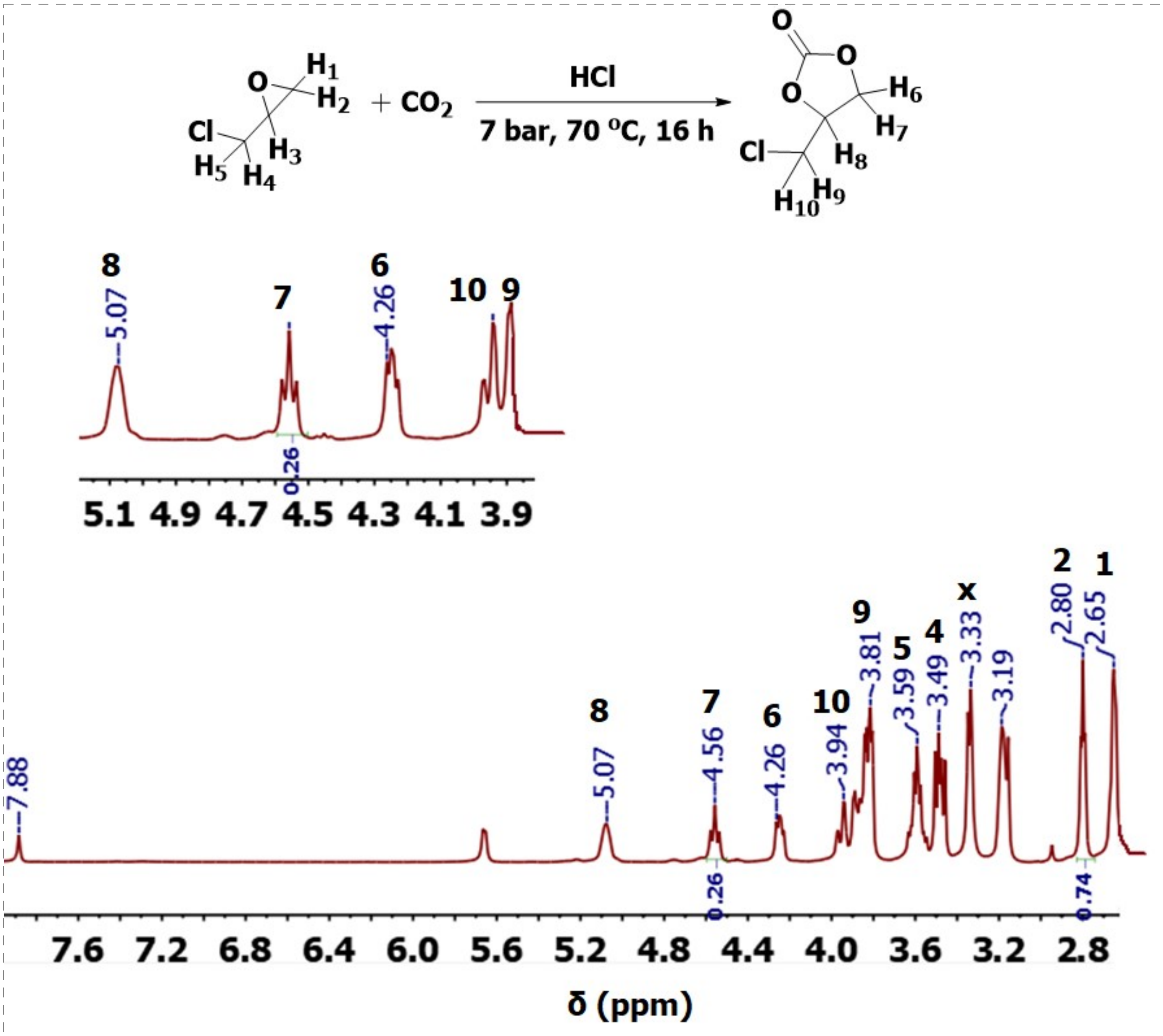

Figure S13. ^{1}H NMR spectrum of ECH conversion in DMSO-d_6, **x**: water. HCl acid promoted the ring opening step upon the formation of halo-alcoholic compounds.[1,2] (**Table 1**, Entry 7).

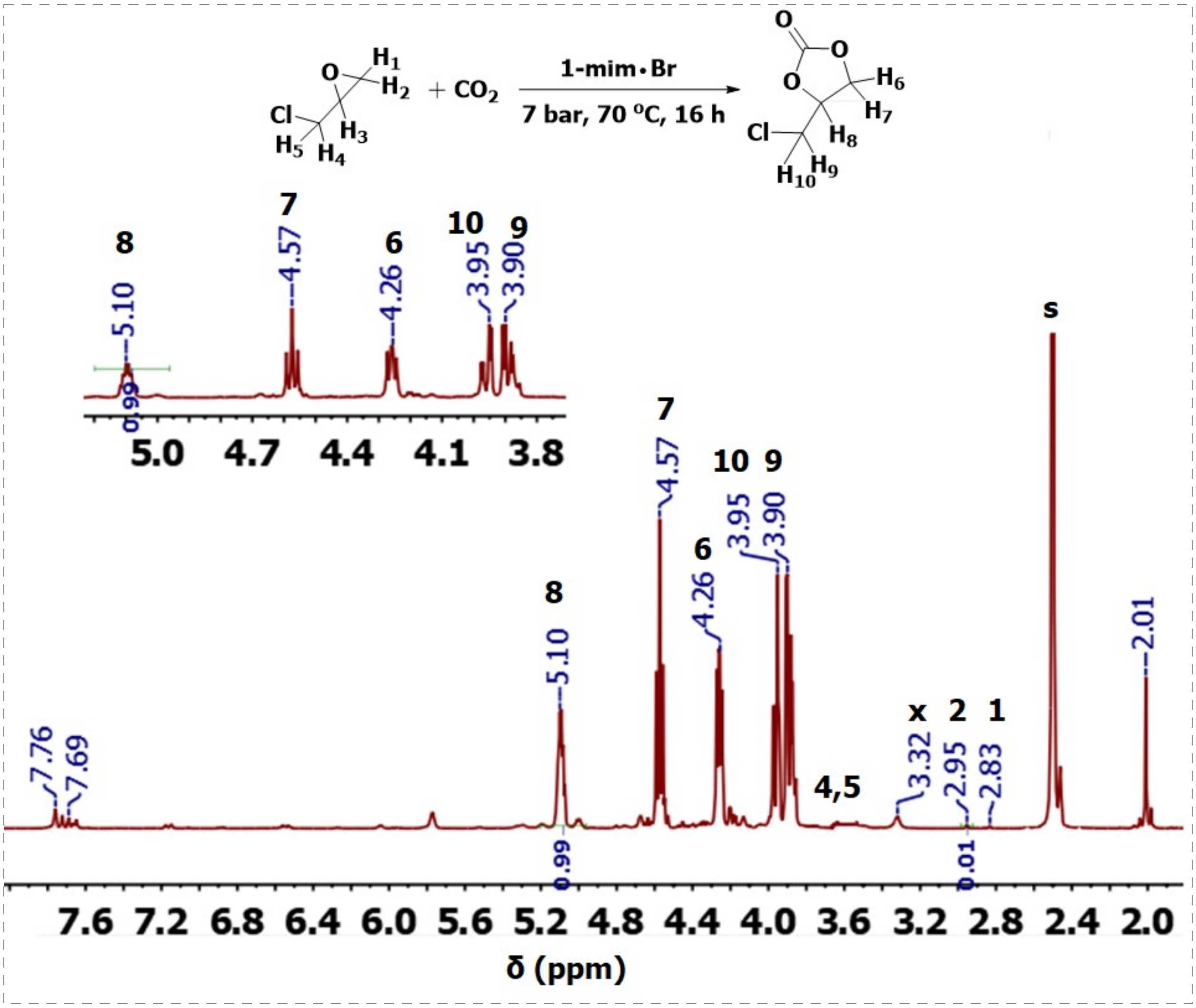

Figure S14. ^{1}H NMR spectrum of ECH conversion in DMSO-d_6, **s**: solvent, **x**: water (**Table 1**, Entry 8).

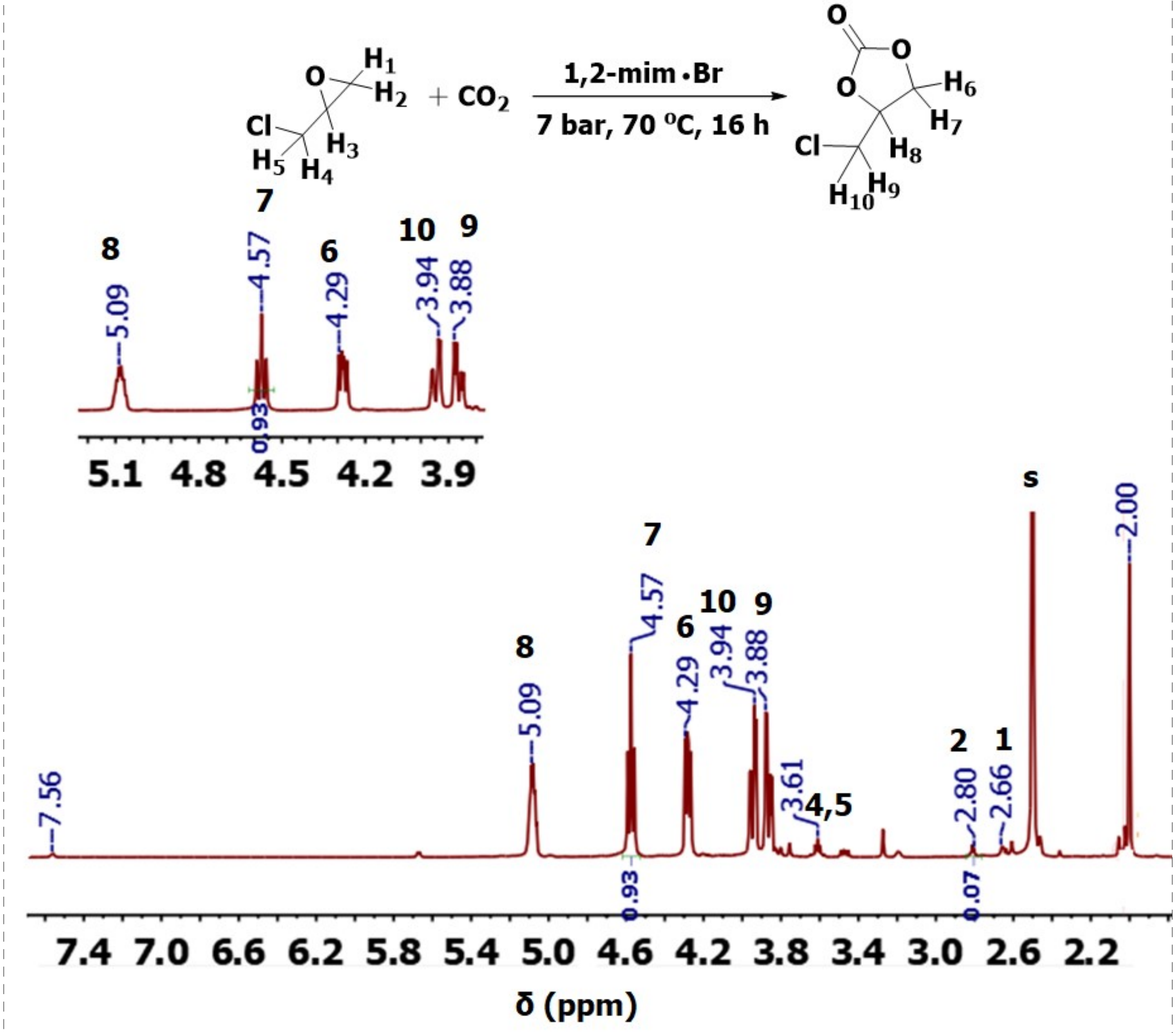

Figure S15. [1]H NMR spectrum of ECH conversion in DMSO-d_6, **s**: solvent, **x**: water (**Table 1**, Entry 9).

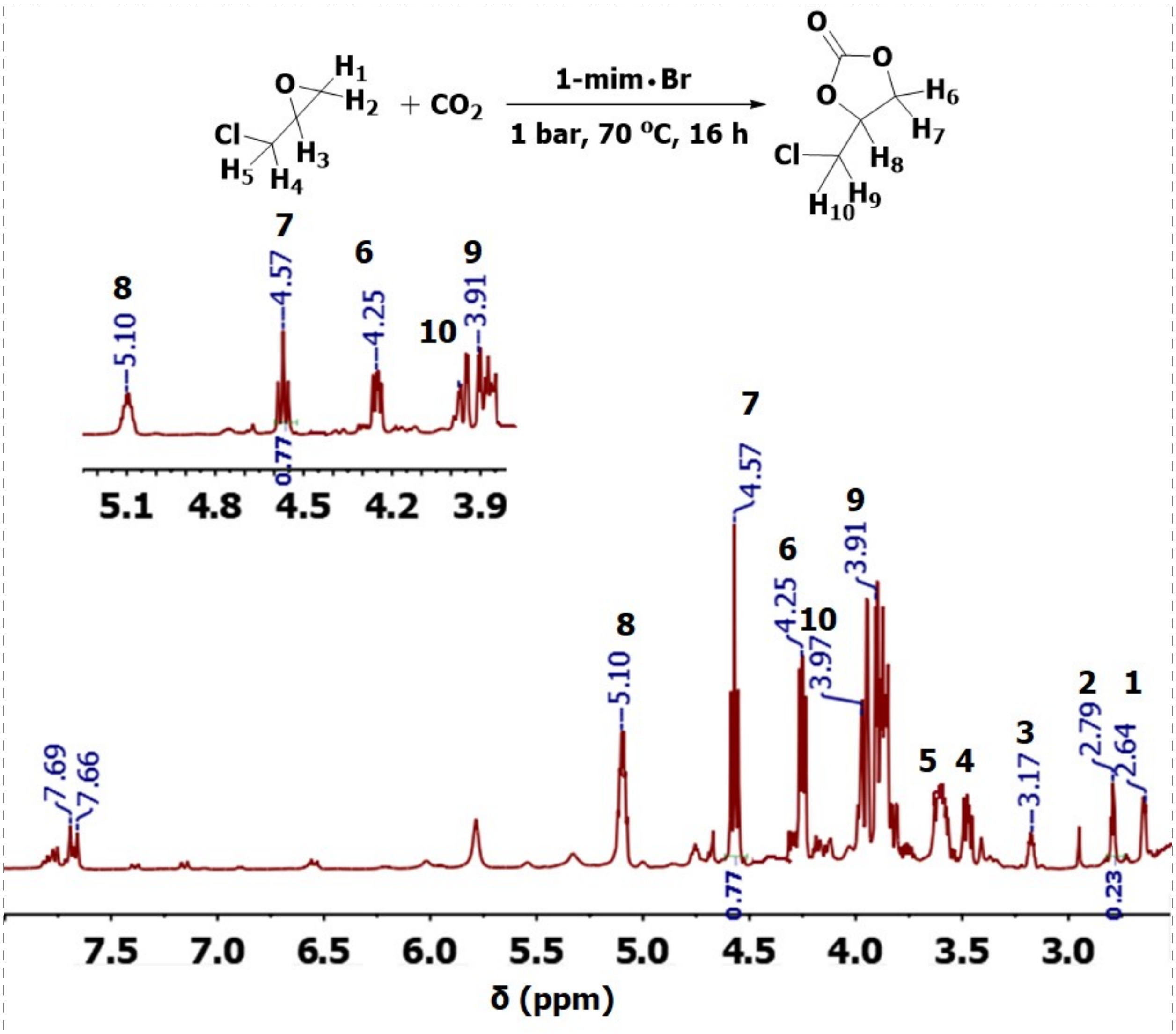

Figure S16. ^{1}H NMR spectrum of ECH conversion in DMSO-d_6 (**Table 1**, Entry 10).

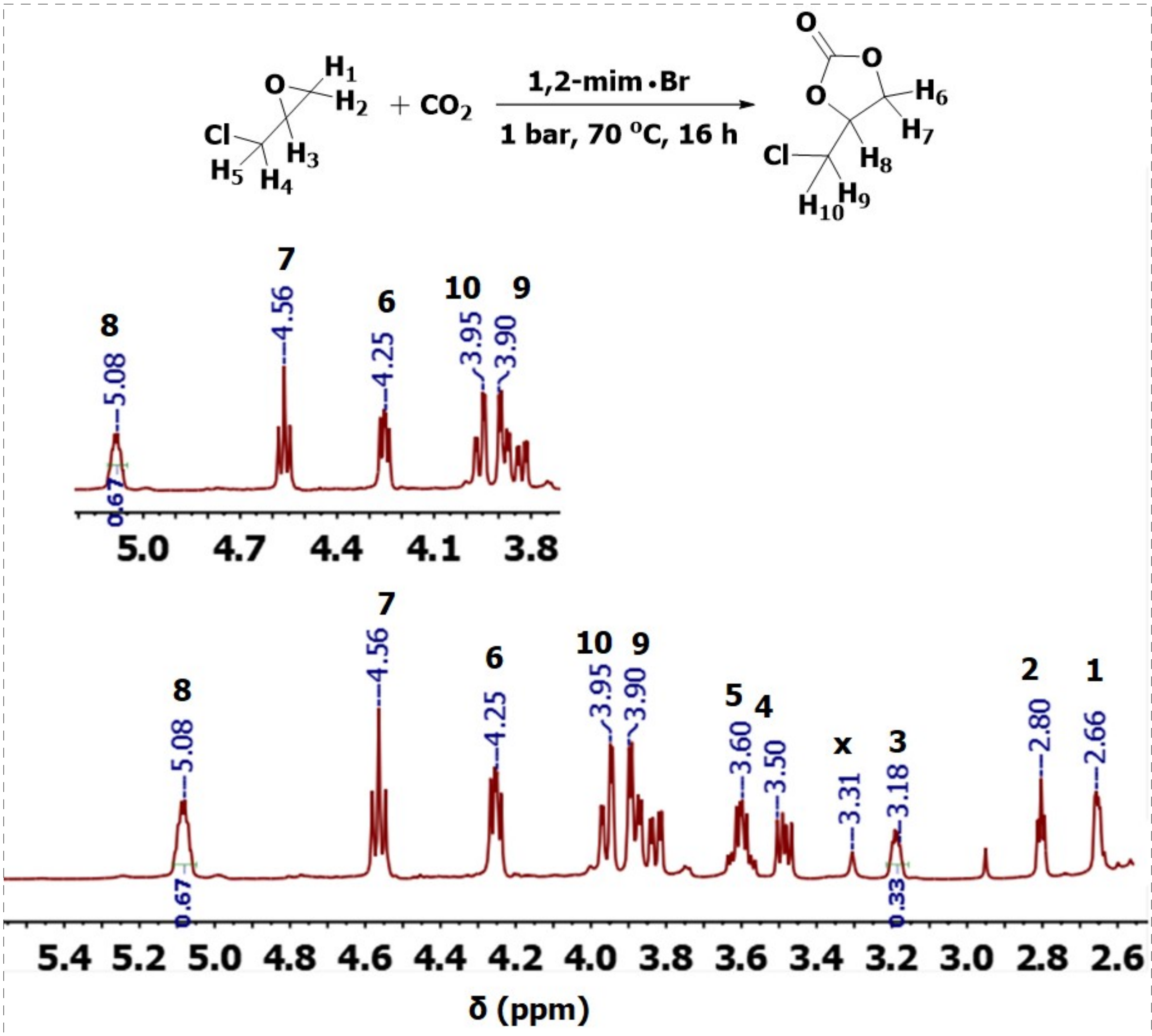

Figure S17. [1]H NMR spectrum of ECH conversion in DMSO-d_6 (**Table 1**, Entry 11).

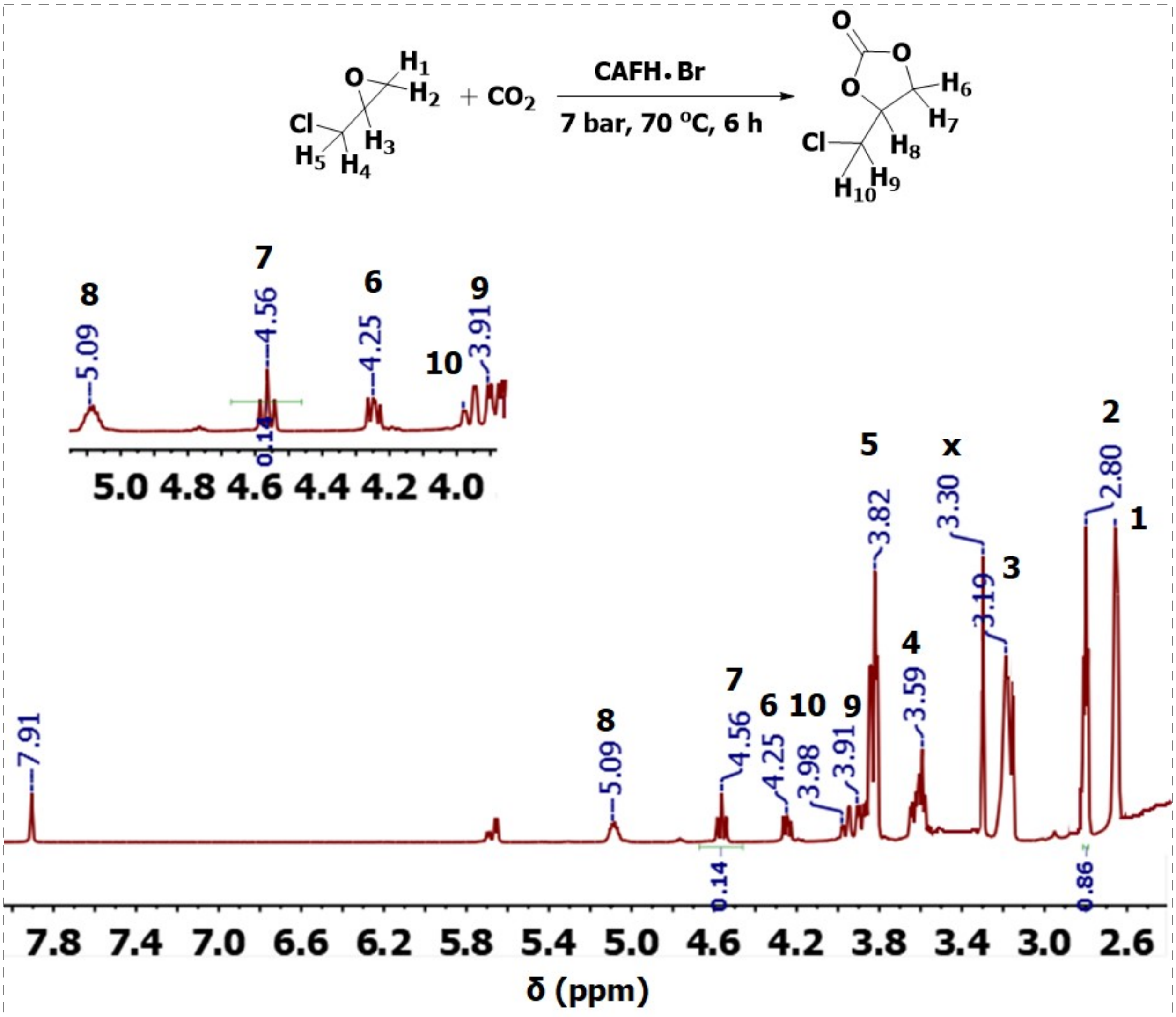

Figure S18. ^{1}H NMR spectrum of ECH conversion in DMSO-d_6 (**Table 2**, Entry 1).

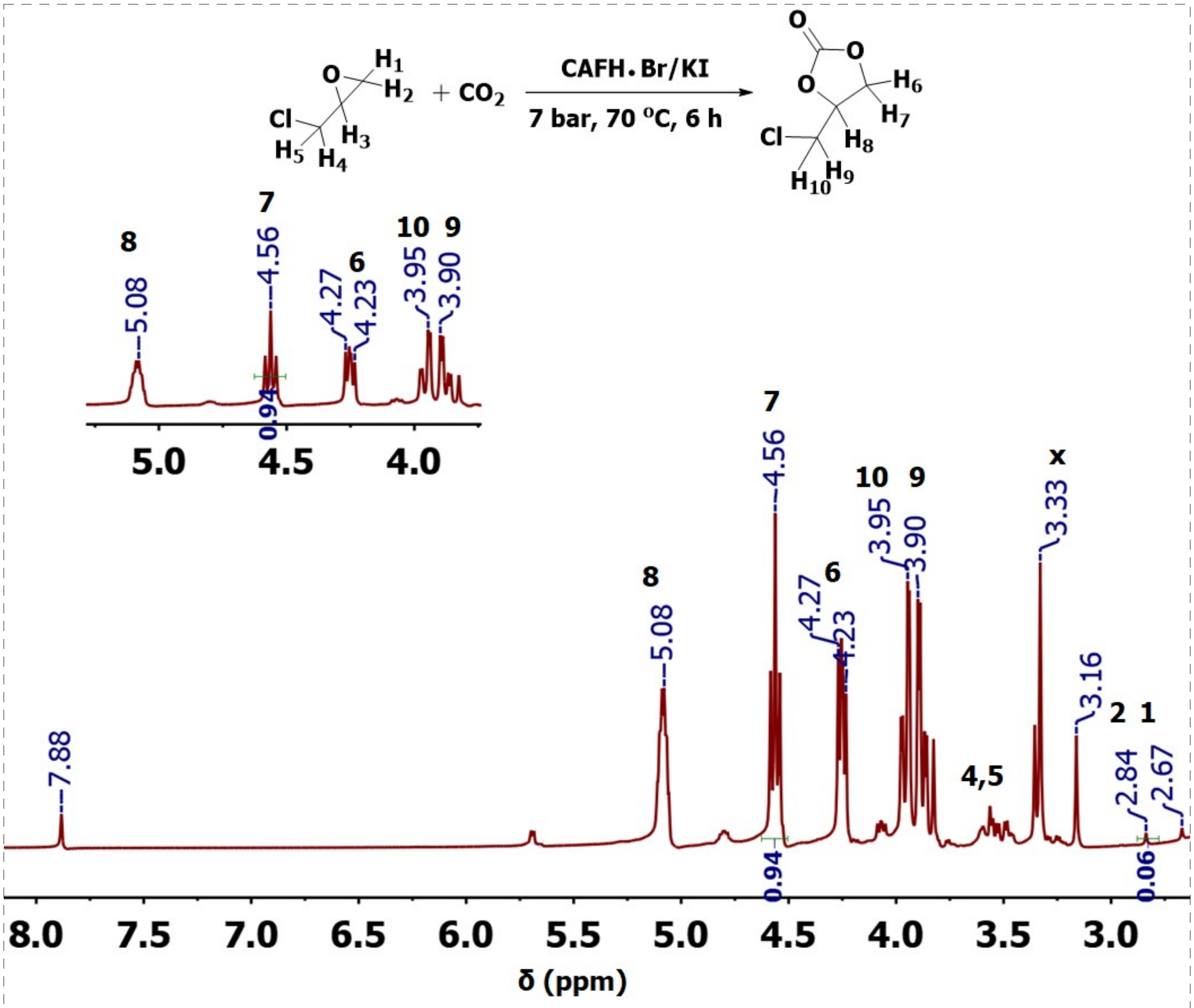

Figure S19. ^{1}H NMR spectrum of ECH conversion in DMSO-d_6 in **CAFH•Br**/KI (1:1, **Table 2**, Entry 2).

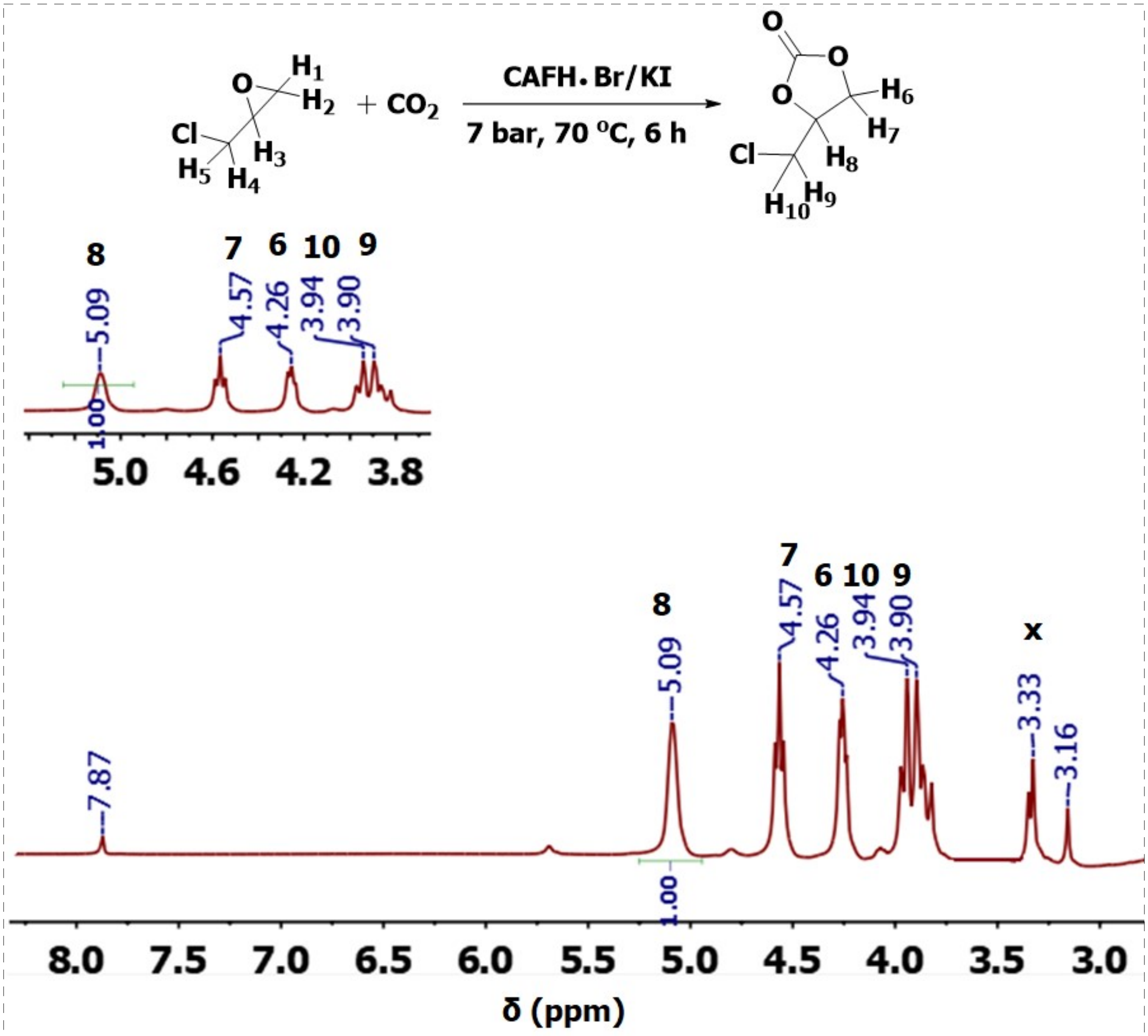

Figure S20. ^{1}H NMR spectrum of ECH conversion in DMSO-d_6 in **CAFH•Br**/KI (1:2, **Table 2**, Entry 2).

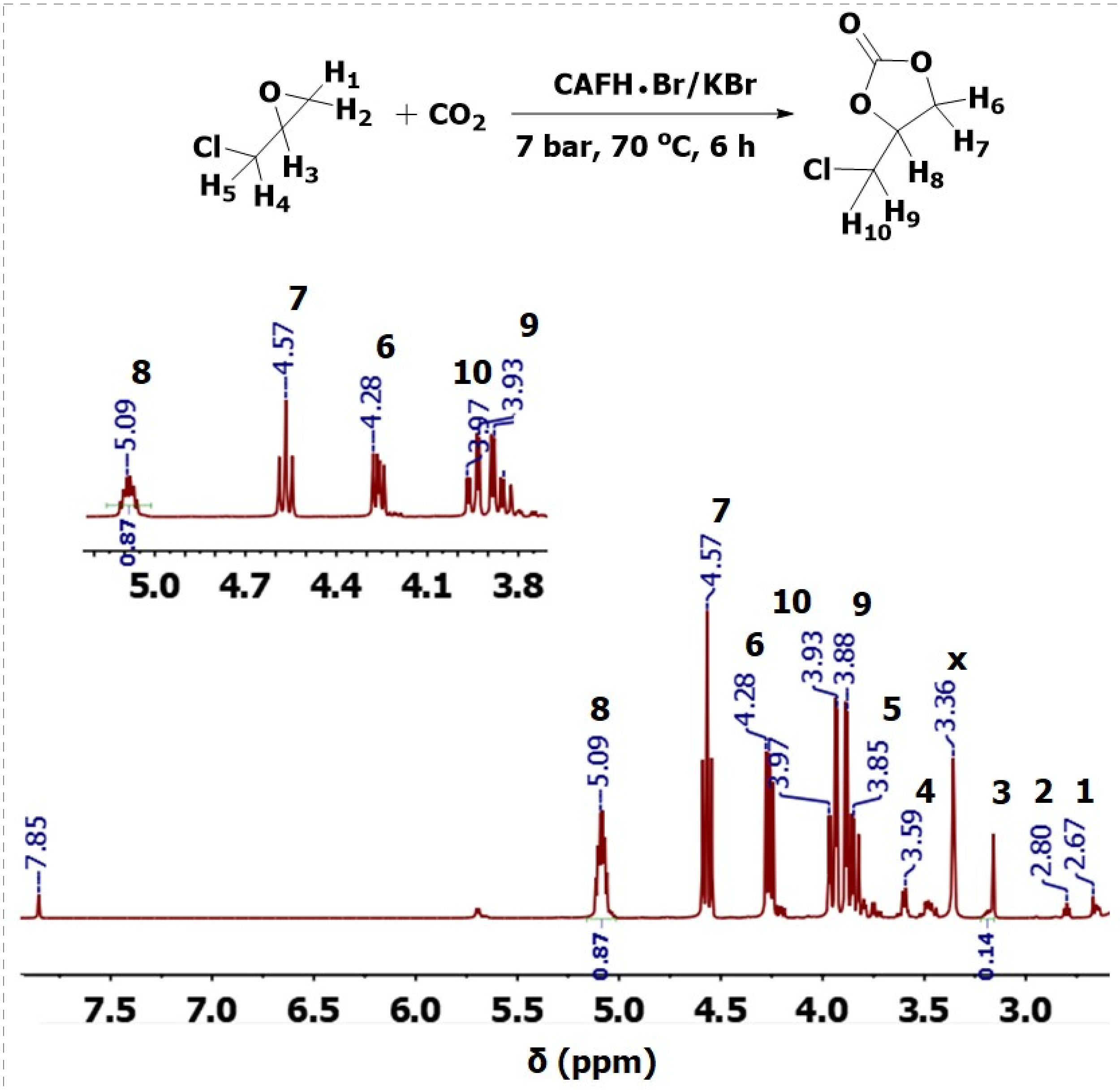

Figure S21. ^{1}H NMR spectrum of ECH conversion in DMSO-d_6 in **CAFH•Br**/KBr (1:1, **Table 2**, Entry 3).

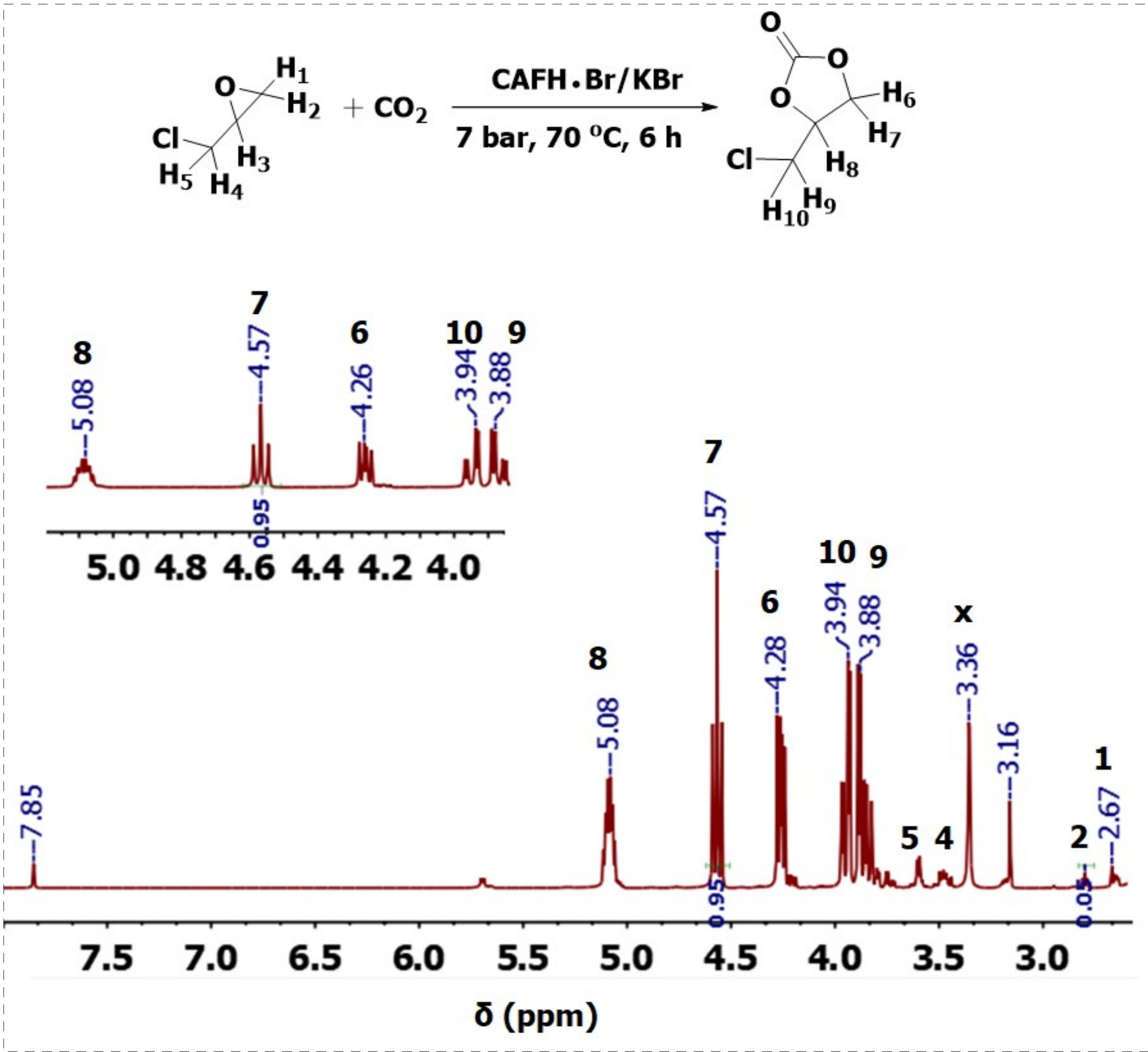

Figure S22. ^{1}H NMR spectrum of ECH conversion in DMSO-d_6 in **CAFH•Br**/KBr (1:2, **Table 2**, Entry 3).

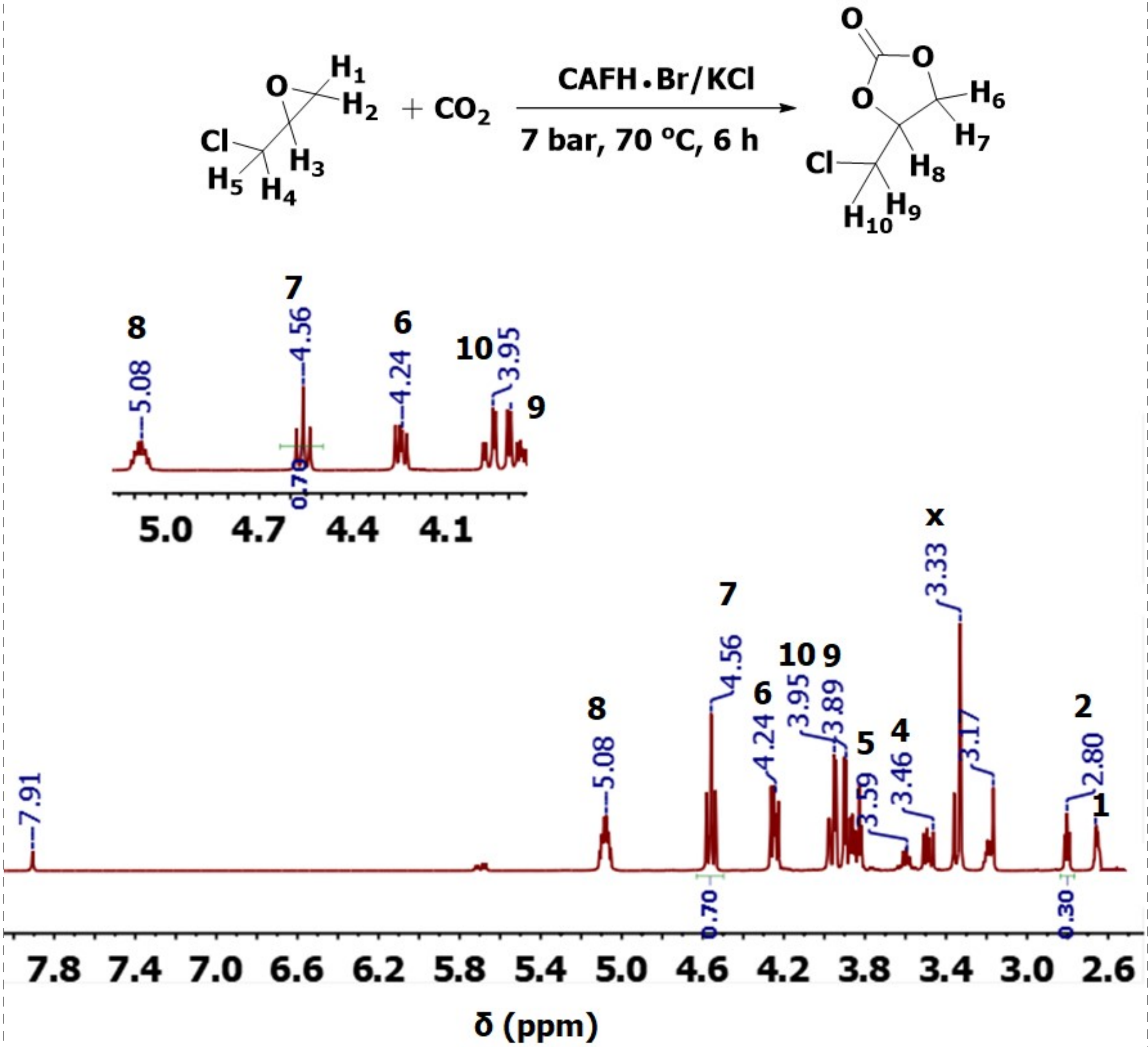

Figure S23. ^{1}H NMR spectrum of ECH conversion in DMSO-d_6 in **CAFH•Br**/KCl (1:1, **Table 2**, Entry 4).

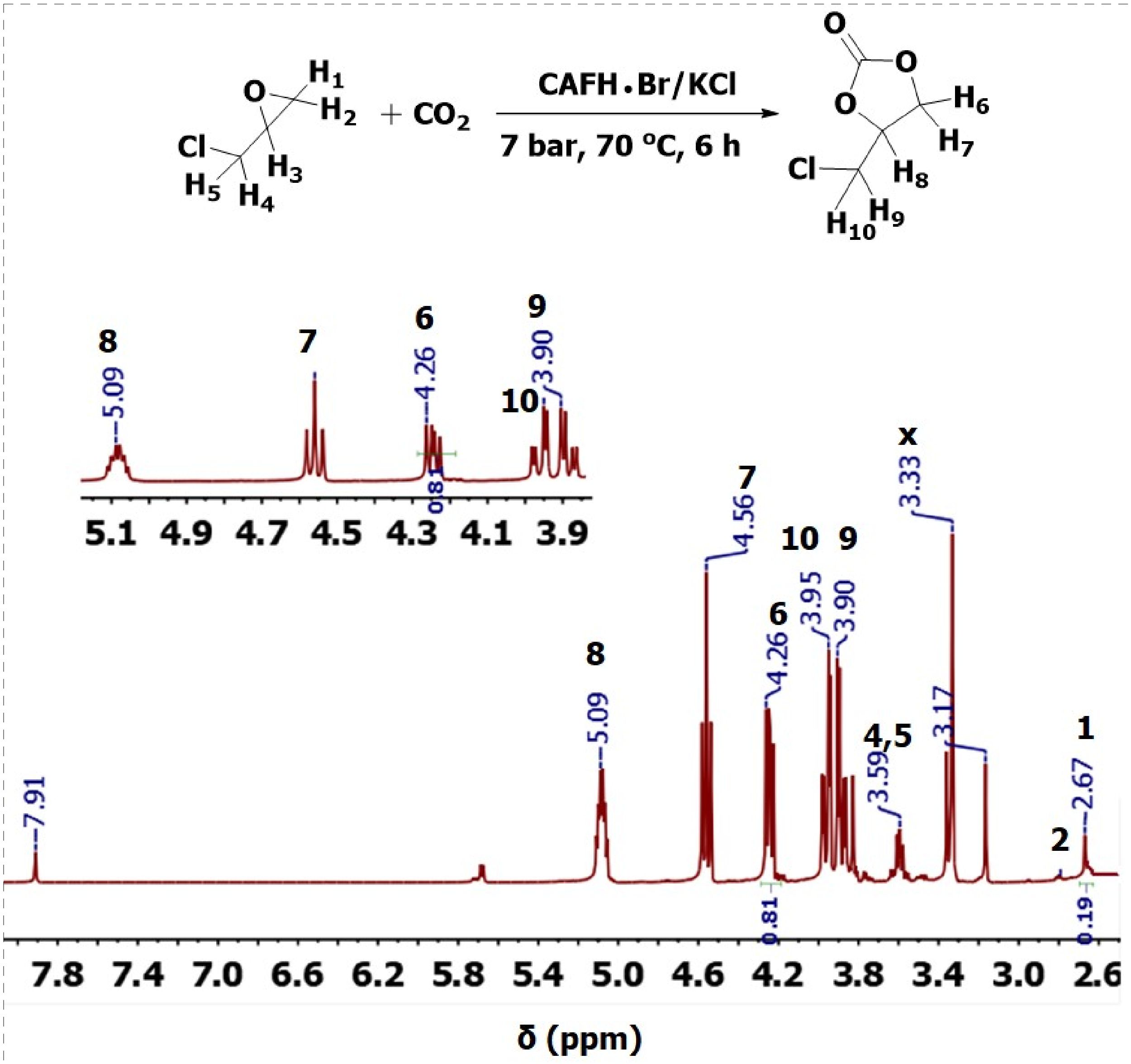

Figure S24. ^{1}H NMR spectrum of ECH conversion in DMSO-d_6, **x**: water, in **CAFH•Br**/KCl (1:2, **Table 2**, Entry 4).

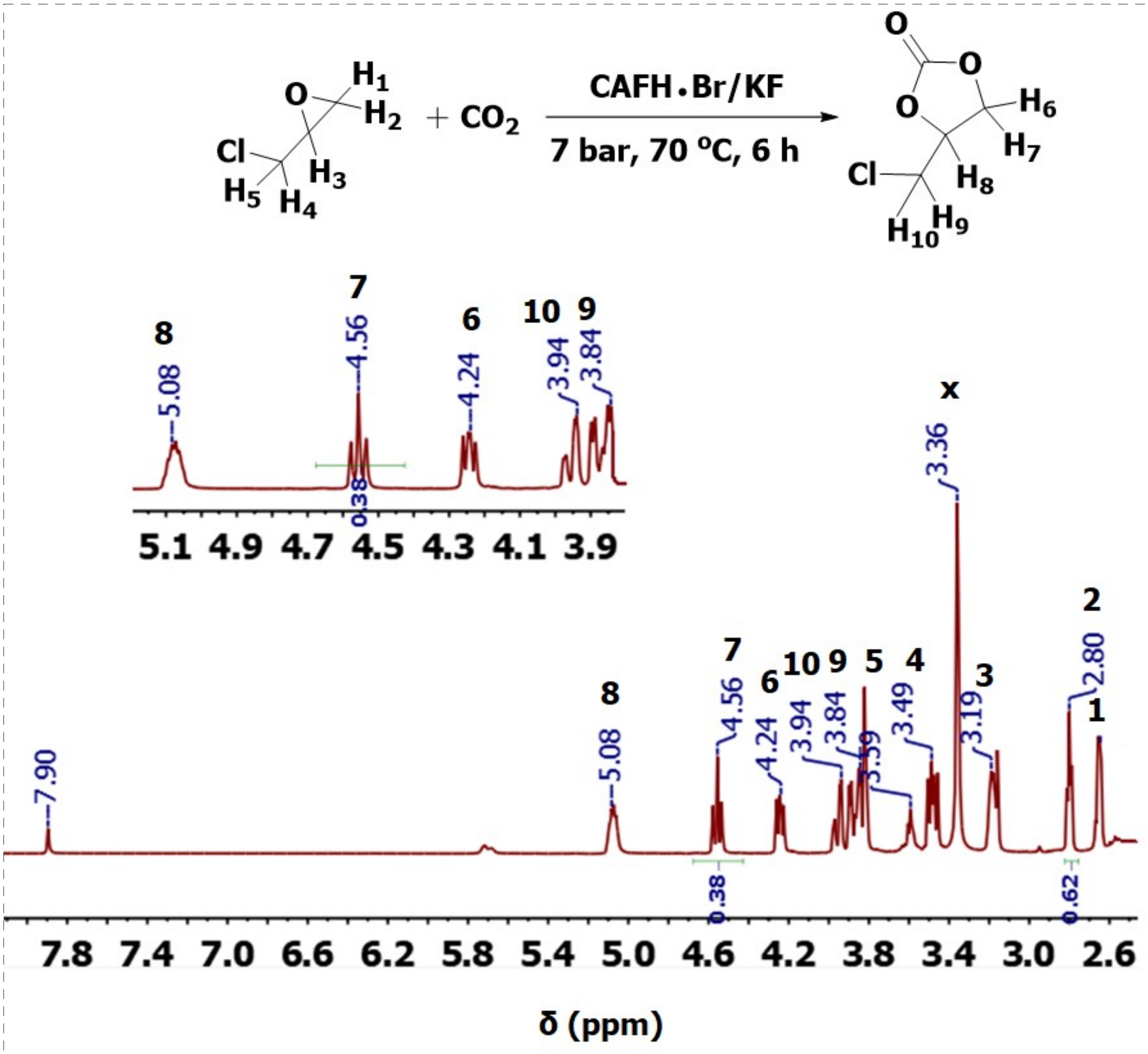

Figure S25. ^{1}H NMR spectrum of ECH conversion in DMSO-d_6, **x**: water, in **CAFH•Br**/KF (1:1, **Table 2**, Entry 5).

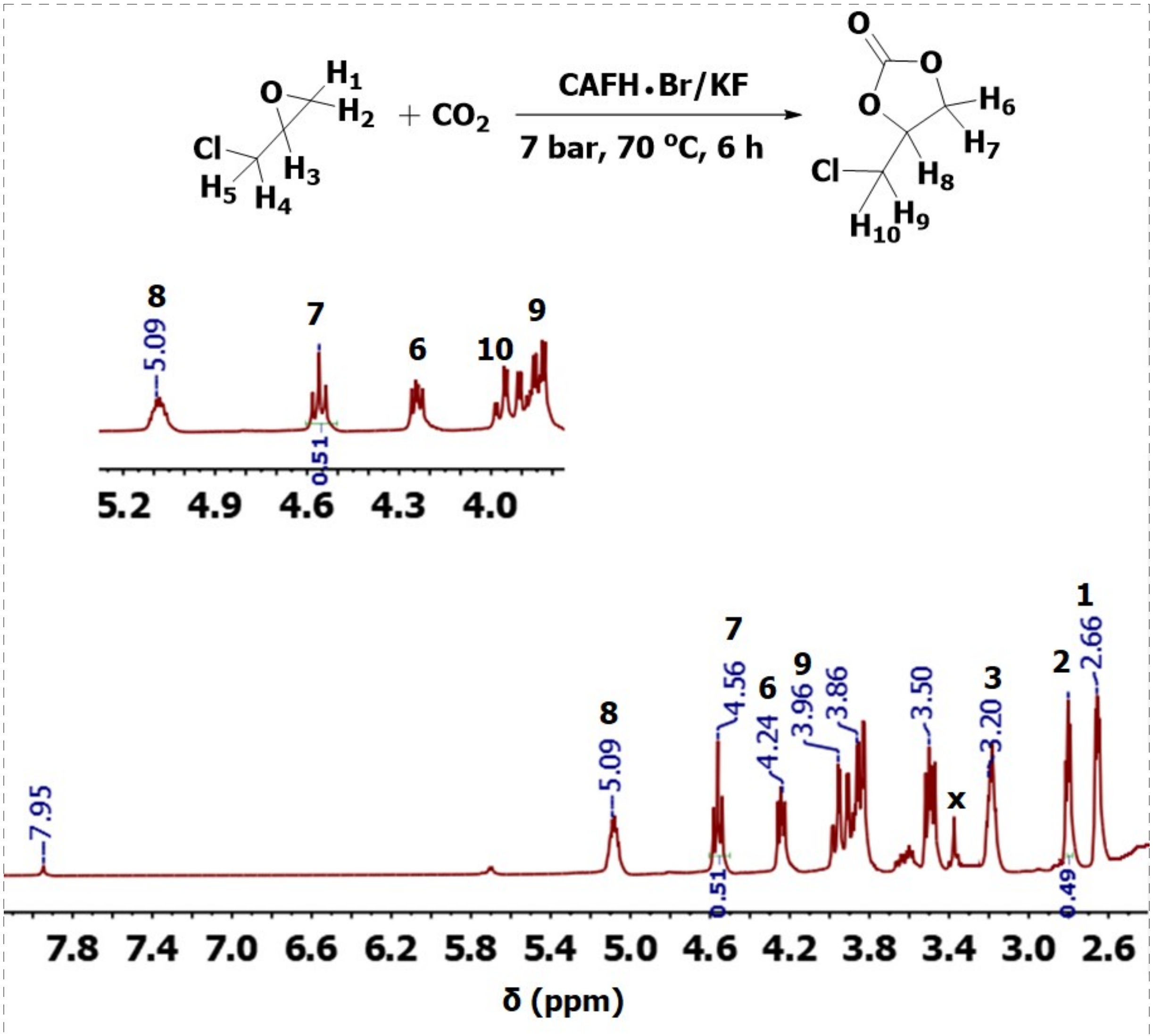

Figure S26. ^{1}H NMR spectrum of ECH conversion in DMSO-d_6, **x**: water in **CAFH•Br**/KF (1:2, **Table 2**, Entry 5).

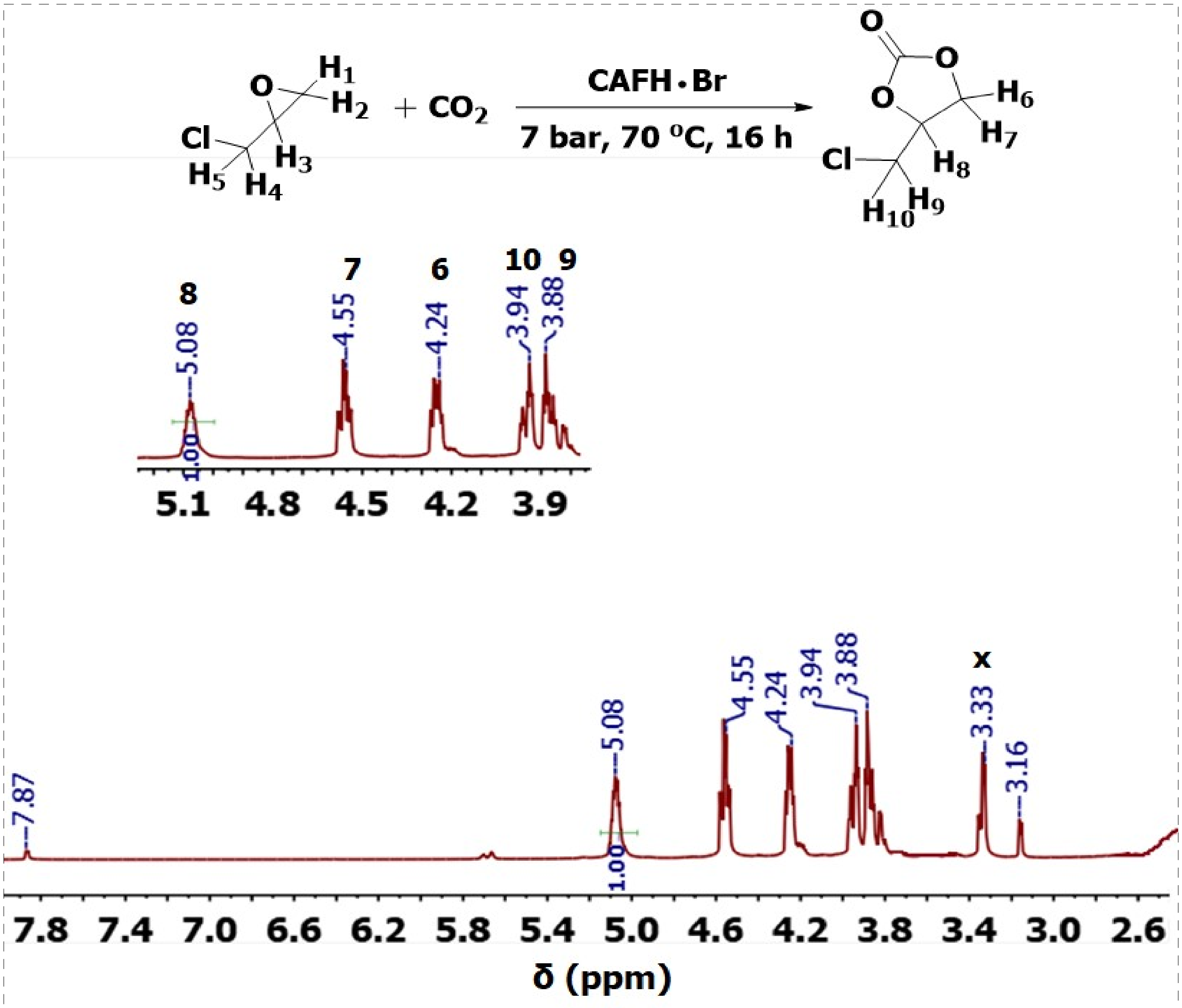

Figure S27. ^{1}H NMR spectrum of ECH conversion in DMSO-d_6 catalyzed by **CAFH•Br**, **x**: water, the peaks at 7.87 ppm corresponding to the catalyst (**Table 3**, Entry 1).

Figure S28. [1]H NMR spectrum of ECH conversion in DMSO-d_6 catalyzed by **CAFH•Br**/KI, **x**: water, the peaks at 7.87 ppm corresponding to the catalyst (**Table 3**, Entry 1).

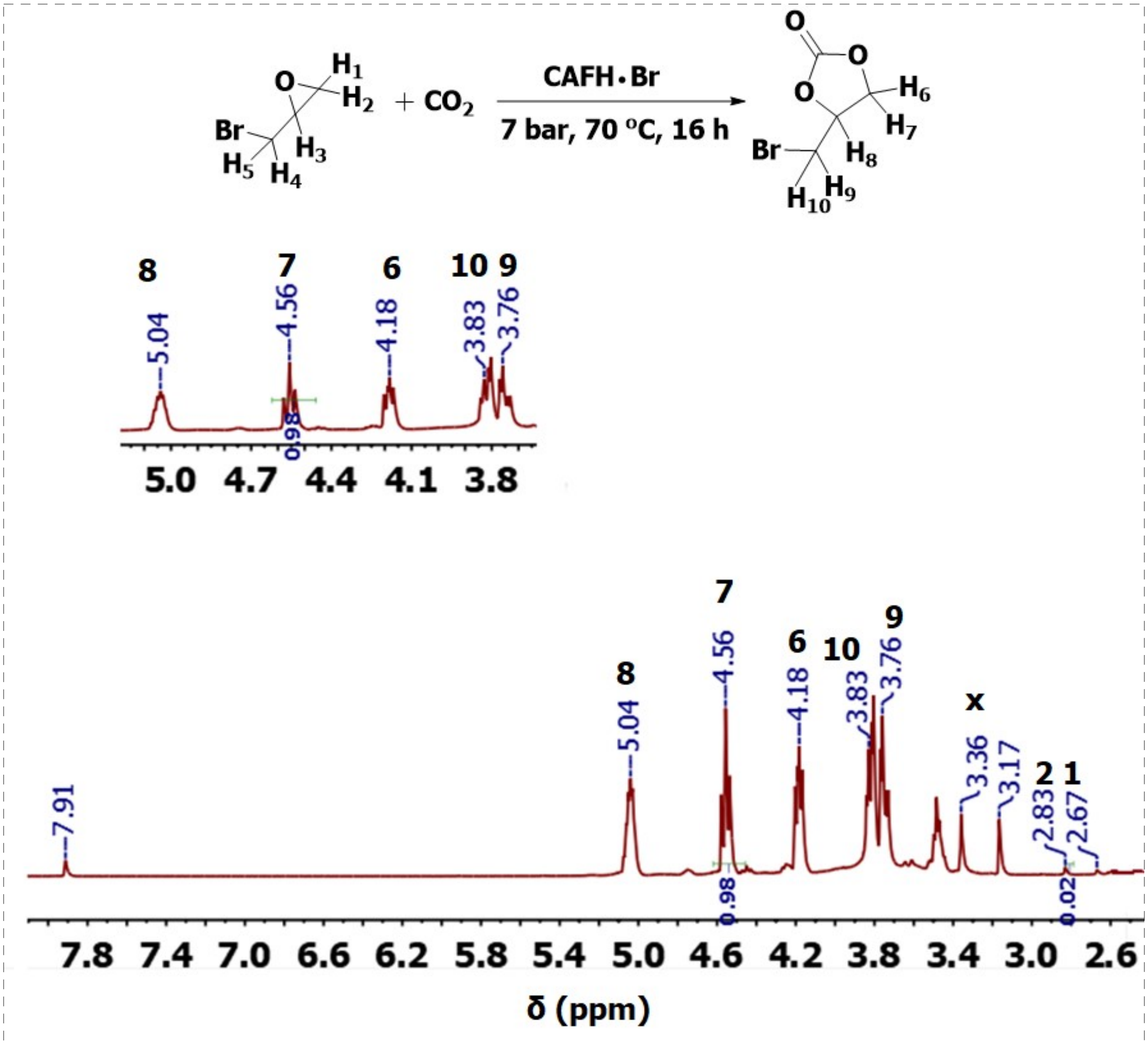

Figure S29. ^{1}H NMR spectrum of EBH conversion in DMSO-d_6 catalyzed by **CAFH•Br**, **x**: water, peaks at 3.17 and 7.91 ppm are corresponding to the catalyst (**Table 3**, Entry 2).

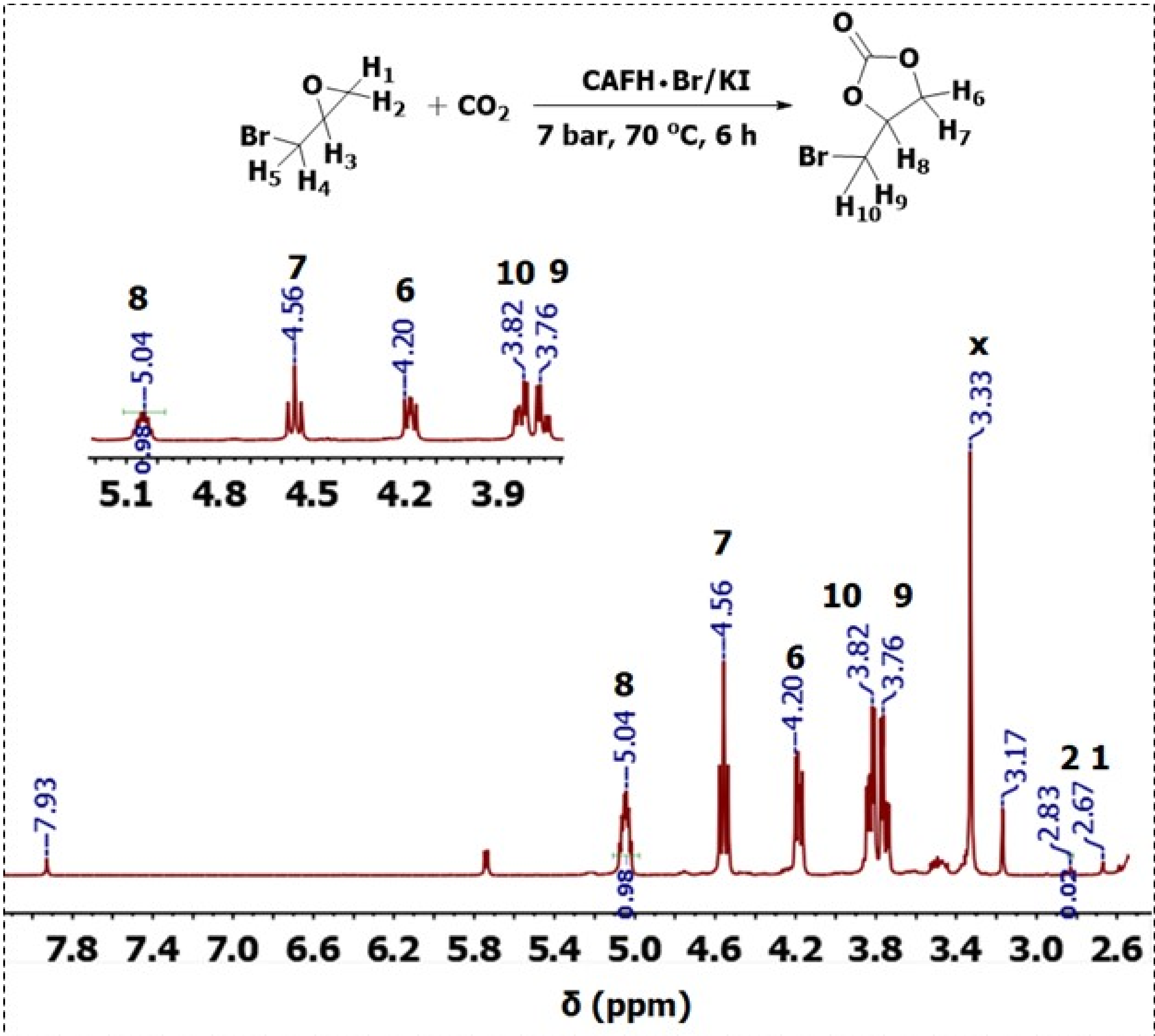

Figure S30. ^{1}H NMR spectrum of EBH conversion in DMSO-d_6 catalyzed by **CAFH•Br**/KI, **x**: water, peaks at 3.17 and 7.93 ppm are corresponding to the catalyst (**Table 3**, Entry 2).

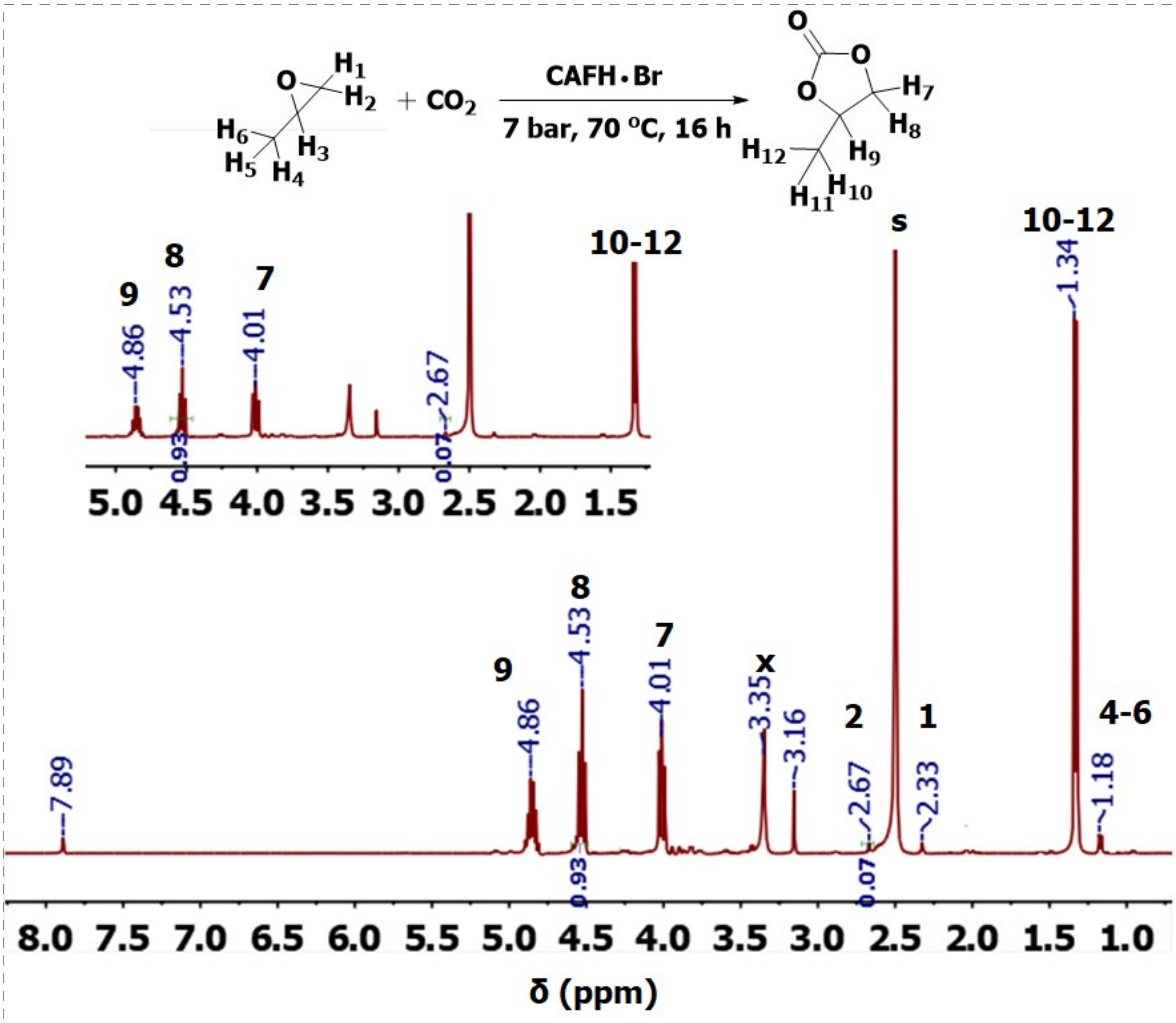

Figure S31. ^{1}H NMR spectrum of PO conversion in DMSO-d_6 catalyzed by **CAFH•Br**, **s**: solvent, **x**: water, peaks at 3.16 and 7.89 ppm are corresponding to the catalyst (**Table 3**, Entry 3).

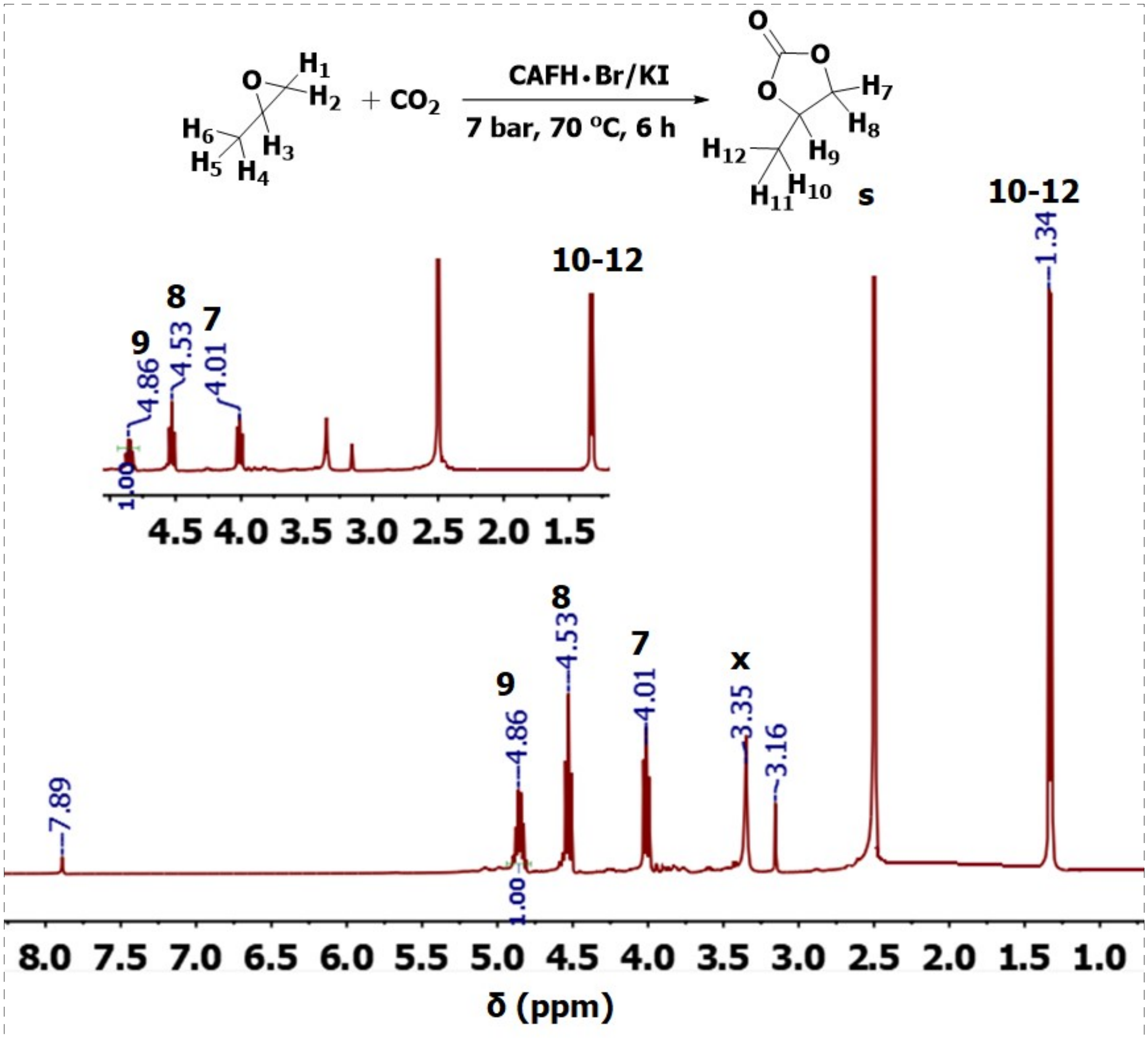

Figure S32. ^{1}H NMR spectrum of PO conversion in DMSO-d_6 catalyzed by **CAFH•Br**/KI, **s**: solvent, **x**: water, peaks at 3.16, 3.82 and 7.89 ppm are corresponding to the catalyst (**Table 3**, Entry 3).

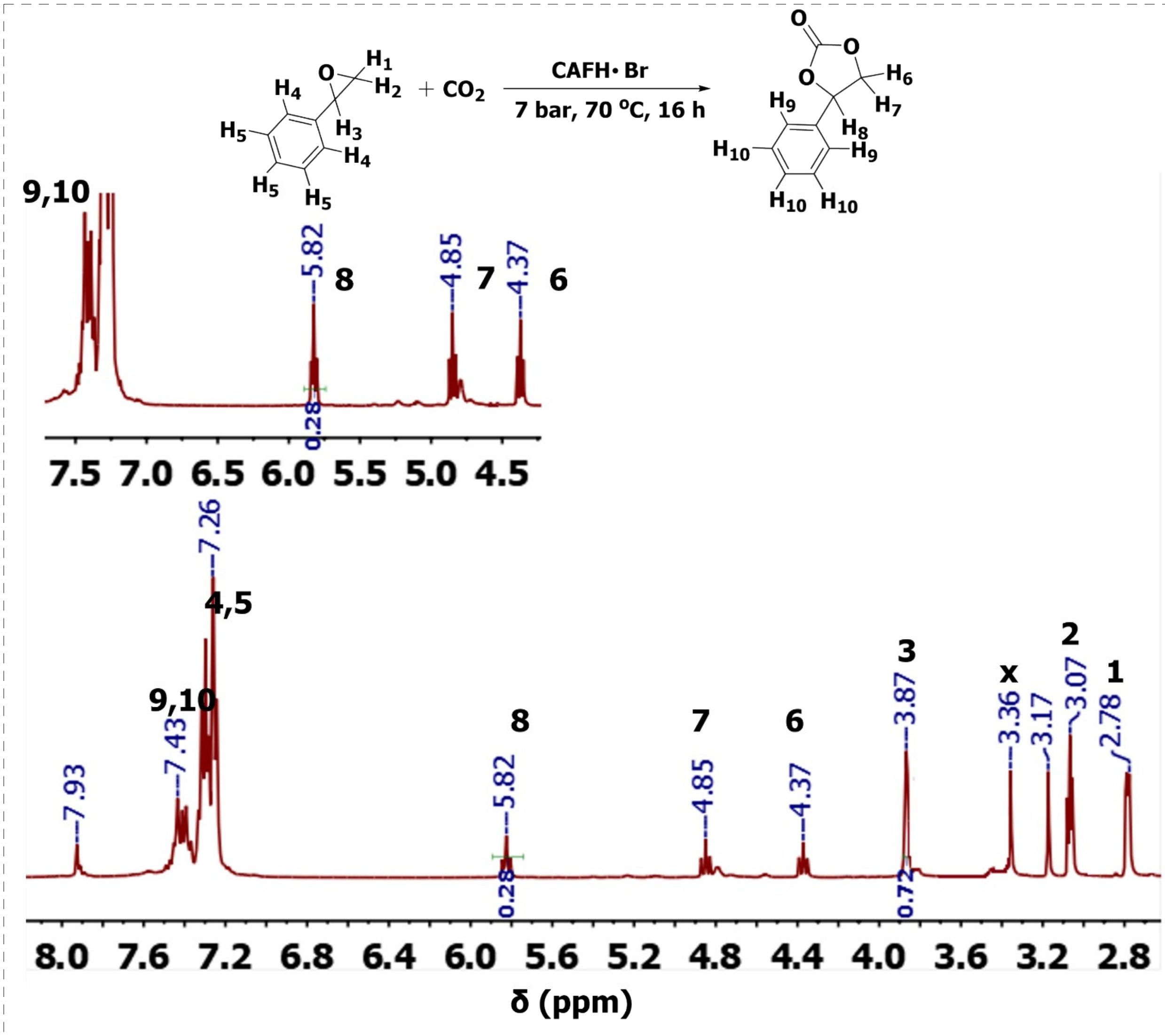

Figure S33. ^{1}H NMR spectra of SO conversion in DMSO-d_6 catalyzed by **CAFH•Br**, **x**: water, peaks at 3.18 and 7.91 ppm are corresponding to the catalyst (**Table 3**, Entry 4).

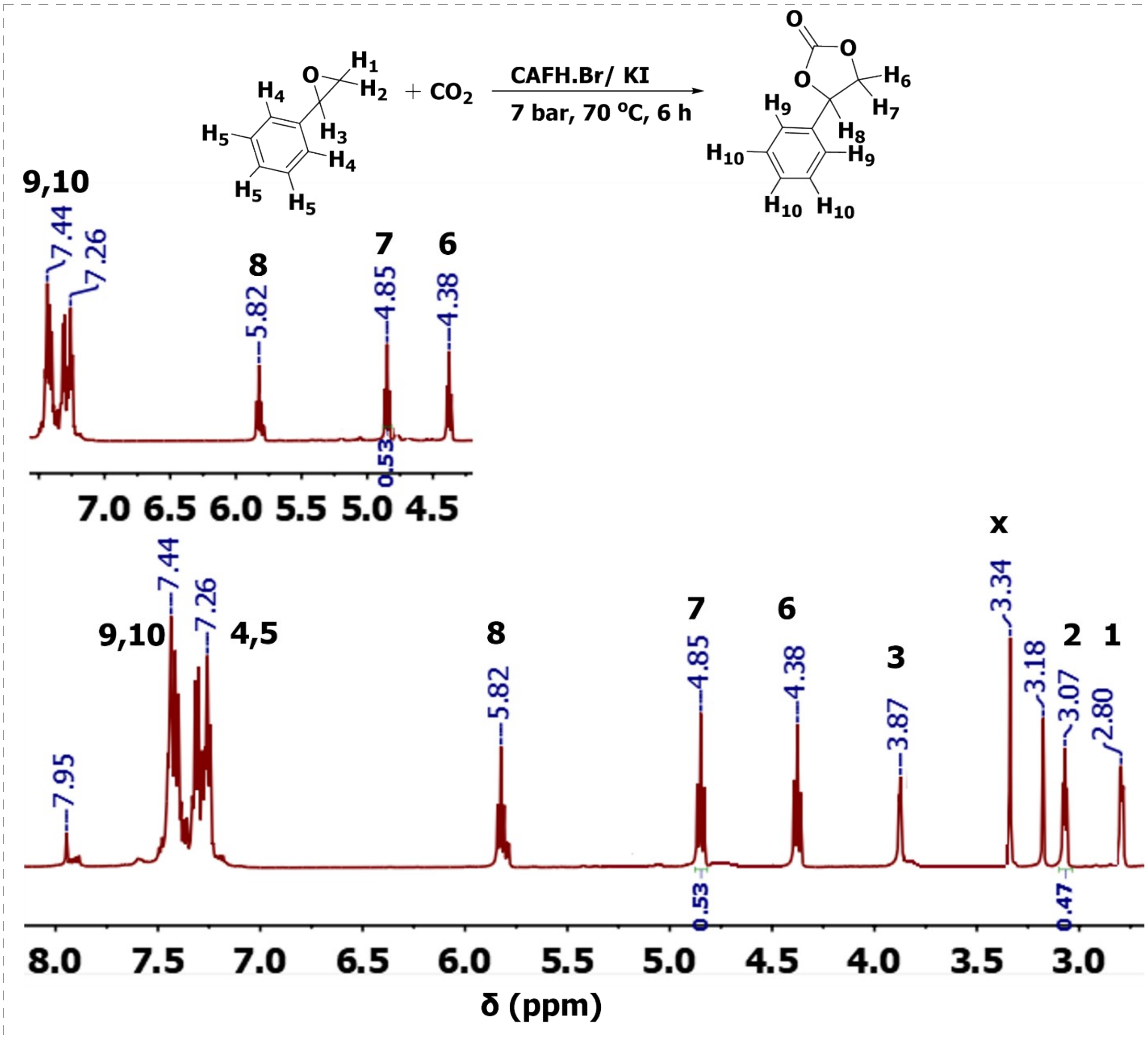

Figure S34. [1]H NMR spectrum of SO conversion in DMSO-d_6 catalyzed by **CAFH•Br**/KI, **x**: water, peaks at 3.17 and 7.93 ppm are corresponding to the catalyst (**Table 3**, Entry 4).

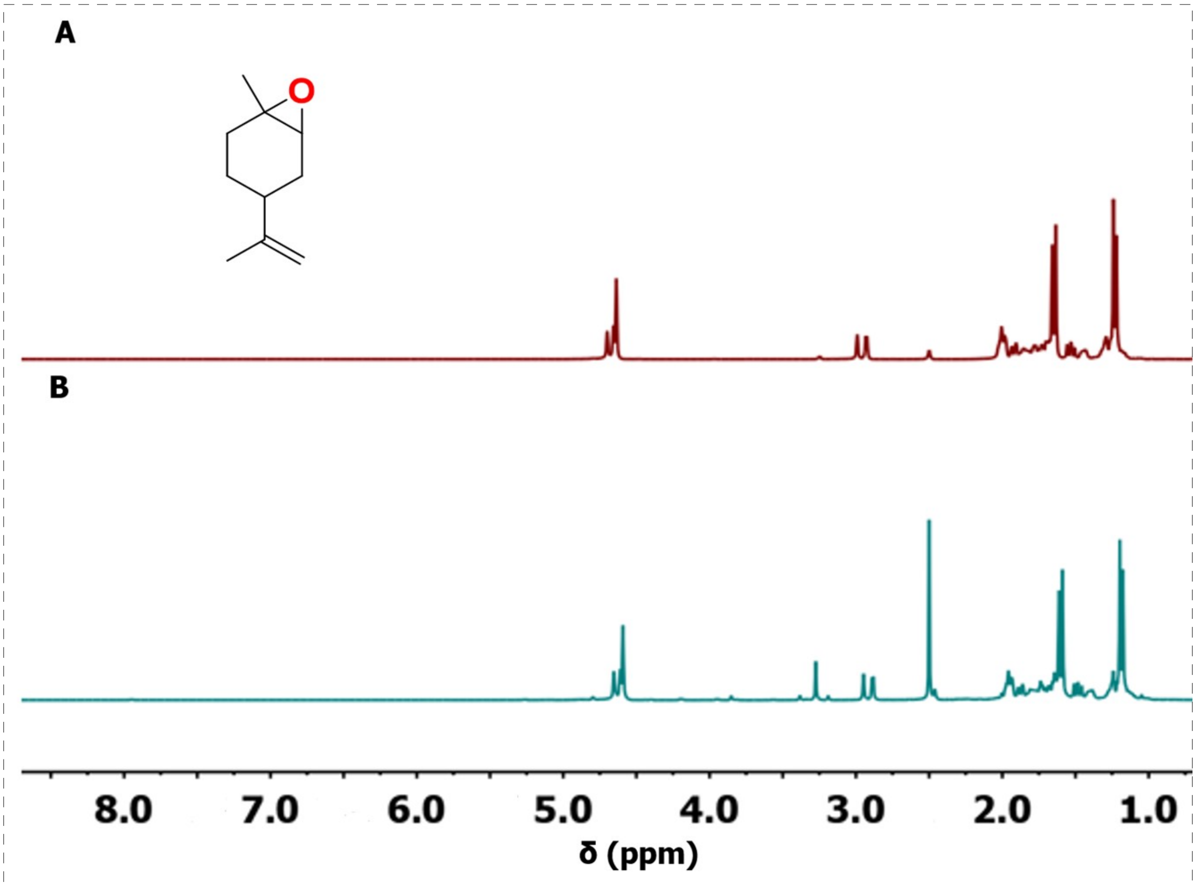

Figure S35. ^{1}H NMR spectra in DMSO-d_6 of: **A.** LO (maroon trace); **B.** LO coupled with CO_2 (blue trace) in the presence of **CAFH•Br**/KI. The cyclic carbonate peaks are not observed (**Table 3**, Entry 5).

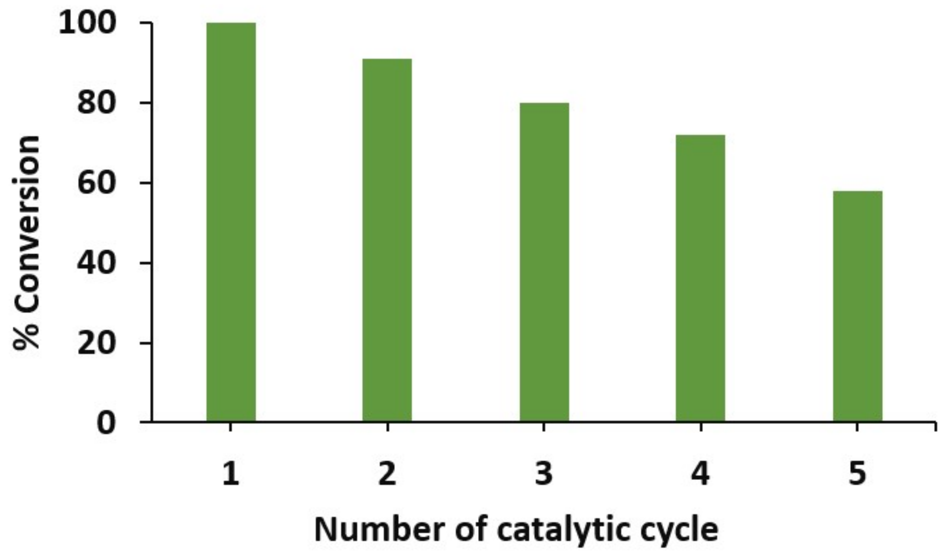

Figure S36. Reusability of **CAFH•Br** over five catalytic cycles. The linear decrease in catalytic activity was anticipated to losses during catalyst separation and filtration.

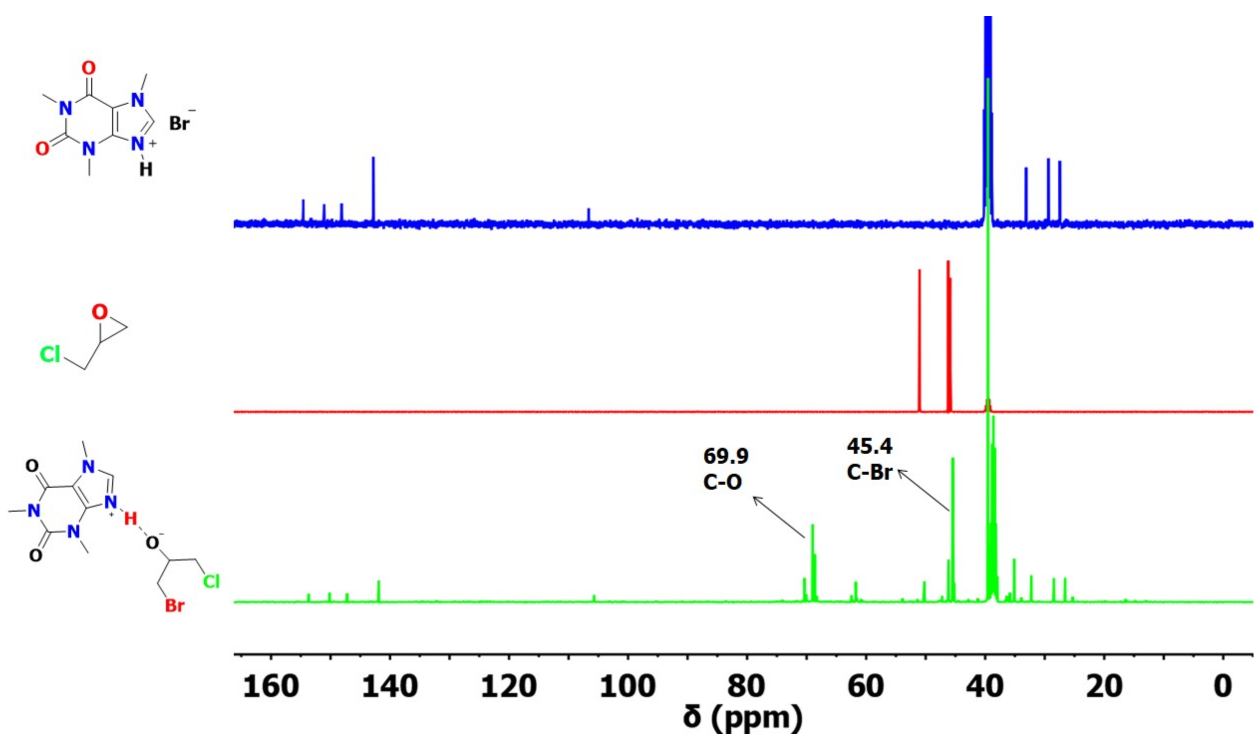

Figure S37. [13]C NMR spectra of CAFH•Br (blue trace), unreacted ECH (red traces), and **CAFH•Br**/ring opened ECH under N_2 atmosphere (green trace) in DMSO-d_6.

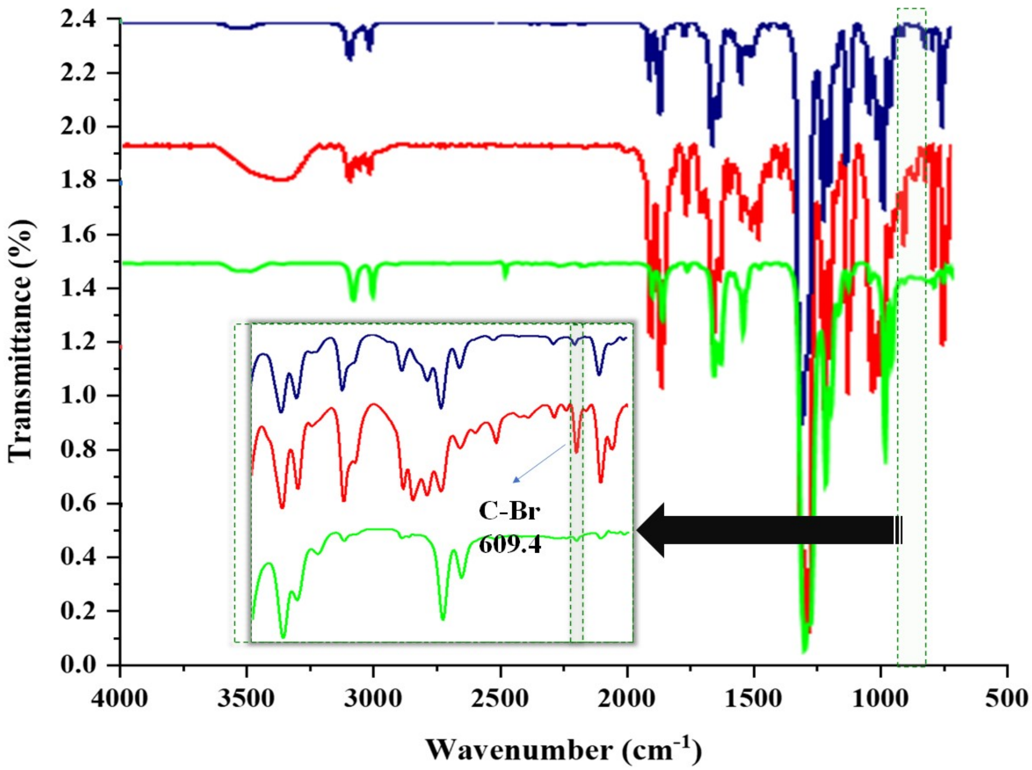

Figure S38. ATR-FTIR of the original mixture (blue traces), spectrum showed C-Br bond upon the alkoxide formation (red traces), spectrum showed C-Br bond disappearing upon bubbling with CO_2 (green traces).

References

1 W.-M. Ren, Y. Liu and X.-B. Lu, *J. Org. Chem.*, 2014, **79**, 9771–9777.
2 S. Biswas, D. Roy, S. Ghosh and S. M. Islam, *J. Organomet. Chem.*, 2019, **898**, 120877.